UNIVERSITÀ DEGLI STUDI DI PALERMO
Dottorato di ricerca in Oncologia e Chirurgia Sperimentali
Dipartimento di Discipline Chirurgiche Oncologiche e Stomatologiche (Di.Chir.On.S.)

Immunological micro and macroenvironment modifications for the early diagnosis and prognostication of breast and prostate adenocarcinomas

Doctoral Dissertation of:
Valeria Cancila

Tutor:
Prof. Claudio Tripodo

The Chair of the Doctoral Program:
Prof. Antonio Russo

2016/2018 – Cycle XXXI

INDEX

Abstract

Cancerogenesis represents the outcome of a dynamical and reciprocal interaction among transforming cells and surrounding microenvironment. It is commonly accepted this interplay contributes to development and progression of cancer and influences the malignant phenotype. Cross-communication among these components is driven by tumor-derived soluble factors and may promote carcinogenesis through the recruitment of stromal and immunological components into the tumor site. To better understand how these dynamics control the transition from pre-malignant lesions to cancer, we focus on the involvement of micro and macroenvironment. Specifically, we investigated the immunosuppressive role of mast cells in promoting immune tolerance and supporting tumor growth. Then, we studied the macroenvironmental modifications within the hematopoietic bone marrow since the early-stages of carcinogenesis.

Summary

One of the most critical issues in cancer is an advanced-stage diagnosis that decreases the chance of successful treatments. The results obtained in the last recent years allowed to improve earlier cancer diagnosis and develop new therapeutic strategies.

Carcinogenesis is a heterogeneous environment populated by innate and adaptive immune cells and stromal components that, through the release of soluble mediators, can promote tumor proliferation, apoptosis resistance, vascular permeability, angiogenesis and metastases. Defective stress response during tissue homeostasis create permissive conditions for tumor growth through chronic exposure to cell survival signals, proangiogenic and anti-DNA repair factors, extracellular matrix-modifying enzymes that increase tumor-promoting inflammatory chemokines and cytokines. In this study we highlight the remodelling of micro and macroenvironment during tumor progression. Assuming that immunological components influence tumor phenotype, growth and invasiveness, in the first part of the study, using the spontaneous prostate cancer TRAMP model, we gained insight into the role of mast cells (MCs) in regulating the balance between tumor-promoting and tumor suppressive events. Specifically, MCs support *in vivo* the growth of prostate adenocarcinoma, whereas their pharmacological targeting through Imatinib favors prostate neuroendocrine (NE) cancer.

Moreover, the immunosuppressive ability of mast cells prompted our investigation on whether MCs support myeloid-derived suppressor cells (MDSC) recruitment within the tumor lesion and their suppressive activity.

Accumulating evidence indicate that beside local modifications, neoplastic cells foster the alterations of the hematopoietic output and favour preferential production of immune cell differentiation towards specific immune-modulatory or pro-inflammatory states. Therefore, in the second part of this study, we investigated the modifications in the bone marrow hematopoietic macroenvironment required to satisfy increased immune cell demand at different stages of tumor development, in spontaneous MMTV-NeuT model of mammary carcinogenesis. Altogether, the experimental results of offer a new insight into the role of immune cells within the microenvironment in influencing tumor phenotype, onset and growth extent sustaining immunosuppression. Moreover, the adaptation of bone marrow hematopoietic macroenvironment during the incipient peripheral transformation allowed us to propose the bone marrow as an early sensor of disease.

CHAPTER 1

Background, Rationale and Objectives

1.1 The tumor microenvironment

One of the most critical issues in cancer is represented by an advanced-stage diagnosis that associates with a decreased survival probability. The results obtained in the last recent years allowed to improve earlier diagnosis of cancer and develop new therapeutic strategies to detect "precancerous disease" before symptoms start [1].

The theory that cancer is composed exclusively by tumour cells has been overcome. It is accepted today that carcinogenesis is not a cell self-governing, but a heterogeneous environment [2], a complex entity populated by different cell types. The tissue microenvironment of developing tumours consists of innate immune cells (neutrophils, macrophages, basophils, eosinophils, mast cells, myeloid derived suppressor cells, dendritic cells and natural killer cells), adaptive immune cells (T and B lymphocytes) and tumour stroma (fibroblasts, vascular components, mesenchymal stromal cells) [3]. Cross-talk between cancer cells and components of the tumour microenvironment (TME) plays a critical role in cancer development, survival, progression, metastasis and resistance to therapy [4]. These different actors can influence cancer phenotype, through the release of soluble mediators that promote tumour cell proliferation, apoptosis resistance, vascular permeability, angiogenesis, migration of other cells into the TME and immune-escaping [5].

Recent findings identify carcinogenesis as a defective stress response during tissue homeostasis, therefore a continuous control of neighboring cells can be as relevant as

the control of cancerous cells [6]. How do tissues maintain homeostasis and, how do cells become transforming cells are major focuses of cancer research.

1.2 Tissue homeostasis alterations

Normal tissue preserves physiologically a stable architecture maintaining a balance between cell-proliferation and death control [7]. The innate and adaptive immune compartments play a crucial role in eliminating damaged, senescent and pre-malignant cells and restoring tissue homeostasis [8]. Dangerous signals identified by pattern recognition receptors (PRRs) trigger immune response and inflammation releasing pro-inflammatory cytokines and chemokines [9,10,11]. Bacterial and viral infections as well as carcinogens cause persistent inflammation and establish tumor-promoting microenvironment through chronic exposure to growth factors, cell survival signals, proangiogenic and DNA repair reduction factors and extracellular matrix-modifying enzymes [12]. Sometimes, this inflammatory status follows oncogenic events as mutations, chromosomal translocations, alterations of proto- or anti-oncogenes, such as in gastrointestinal tumor [13]. In both scenarios, the larger amount of transcription factors such as NF-kB, STAT-3, HIF-1 induces an increase of tumor-promoting inflammatory chemokines and cytokines [13]. By the release of these molecules, the tumor microenvironment controls leukocytes recruitment, activation and proliferation in order to support tumor development or suppress anti-tumor immunity [14]. Also the extracellular matrix (ECM) remodelling, within the TME, is involved in tumor growth. ECM is composed by glycoproteins, proteoglycans, structural proteins such as collagens, laminin and matricellular proteins [15]. The amount, type and distribution of ECM influence tumour progression and dissemination through mechanisms regulating epithelial-to-mesenchymal transition (EMT) [15,16]. Furthermore, the ECM molecules can recruit myeloid cells, suggesting that in the TME an altered ECM deposition may impact the immune cell infiltration. Specifically, deregulated ECM deposition promotes the recruitment of immunosuppressive cells [17] at the tumour site, where they support EMT and metastases [18]. This interplay between ECM composition and myeloid cells denotes a role in determining tumour phenotype and aggressiveness.

A detailed understanding of the TME and the mechanisms linking tumour, stromal and immune cells can contribute to develop efficacious therapeutic strategies and immuno-modulatory approaches.

1.3 Role of mast cells in tumor growth

Mast cells (MCs) are almost ubiquitously distributed among tissues, where they act as a first line of defence against parasitic and bacterial infections [19]. MCs are a key effector in allergic and anaphylactic reactions; their role in IgE-dependent innate immunity is well-known. After allergen-exposure, the binding of antigen-specific IgE antibodies to FcεR expressed on mast cells surface mediate MC degranulation [20].

Yet, MCs participate in inflammation and T-cell mediated immune responses, regulating physiological and pathological conditions [21,22].

MCs play an active role within the TME in regulating the balance between tumor-promoting or inhibitng functions depending on tumor type and localization [23]. Increasing evidence suggest MCs as multifunctional cells intervening in angiogenesis, tissue remodelling, recruitment of immunosuppressive cells and cancer progression [24]. The recruitment, activation and survival of MCs at tumor site are mediated by tumor-released stem cell factor (SCF) and by its receptor c-Kit tyrosine kinase (CD117) expressed on MCs surface [25]. SCF attracts MCs and increases the synthesis and release of several mediators including vascular endothelial growth factor (VEGF), fibroblast growth factor-2 (FGF-2), transforming growth factor beta (TGF-β), IL-8 [26]. The relationship between MCs accumulation and angiogenesis has been described in many types of cancer [27].

MCs also influence extracellular matrix compositions by releasing matrix metalloproteinases (MMPs). In particular, MMP-9 cleaves fibronectin, collagen, elastin, osteonectin [28] and modulates extracellular matrix degradation and promote metastases [29].

More importantly, several findings suggest that MCs exacerbate immunosuppression by inducing anti-tumor T cell tolerance in several diseases, including cancer [30]. MCs interact with regulatory T cells (Tregs) and myeloid-derived suppressor cells (MDSCs) creating a suppressive tumor microenvironment. Specifically, MCs support MDSC

recruitment within the tumor lesion and induce these cells to produce IL-17 that promote Tregs accumulation and their suppressive function [31].

1.4 Cancer immune tolerance

In the recent years, accumulating data show that inflammatory factors released in the TME, are able to revert the immune cell function towards immunosurveillance evasion [32]. In particular, neoplastic cells promote preferential skewing of immune cell functional differentiation towards specific immune-modulatory or pro-inflammatory states [33,34]. These cells display a tolerogenic activity and, recruited to the tumor site, work in concert to establish an immunosuppressive network inhibiting anti-tumor immune responses.

The main cell types involved in establishment and maintenance of peripheral immune tolerance include Tregs, tumor-associated macrophages (TAM), myeloid-derived suppressor cells (MDSCs), tumor-associated dendritic cells (tDCS) and tumor-associated neutrophils (TAN) [35].

$Foxp3^+$ $CD25^+$ $CD4^+$ Treg populations play an essential role in the maintenance of immunological self-tolerance by suppressing a variety of physiological and pathological immune responses against self and non self antigens [36].

TAMs promote angiogenesis, tissue remodelling and metastasis. TAMs generally express of cell surface receptor, secreted cytokines, chemokines and enzymes that inhibit anti-tumor immune responses. For this reason, the count of tumor infiltrating TAMs is associated with poor prognosis [37].

DCs in tumor-bearing hosts actively contribute to tumor evasion of immune surveillance suppressing T cell function through cell-cell interactions and reactive oxygen species releasing [38].

N2-polarized TAN have a protumorigenic phenotype and play a key role in tumor progression promoting angiogenesis, metastases and immune suppression [39].

Functional MDSCs, immature myeloid cells, are one of the principal components of the immunosuppressive microenvironment. They produce a large amount of iNOS or Arginase, which suppress antitumor innate and adaptive immunity T lymphocyte-mediated.

Therefore, cancer exploits immune systems establishing a profound perturbation in myelopoiesis process, providing signals to the bone marrow in order to instruct a hematopoiesis tumor-adapted.

1.5 The Hematopoietic System

Most of the components populating the TME are of hematopoietic origin. The hematopoietic process is primarily based within the bone marrow, a complex tissue lodged within the trabecula bone and tightly regulated through complex gradients among elements of the endosteal compartment, mesenchymal stromal cells, and vascular cells. The interaction between stromal and hematopoietic progenitor and differentiating cells maintains the hematopoietic homeostasis and allows adaptation to perturbing noxae. Hematopoietic stem cells (HSCs) are functionally defined as multipotent cells that restore hematopoiesis if transplanted in patients with ablation of hematopoietic organ [40]. Furthermore, HSCs are characterized by the capabilities of multi-lineage differentiation and self-renewal capacity. After hierarchical differentiation processes, HSCs progressively lose their multipotency ability, replicating or differentiating in Common Lymphoid Progenitor (CLP) or Common Myeloid Progenitor (CMP). CLP can differentiate into T (TCP), B (BCP) and Natural Killer (NKP) cells, whereas CMP give rise to granulocytes (GP), monocytes (MP), erythrocytes (EP) and megakaryocytes (MkP) [41,42]. This mechanism must be highly efficient, plastic and regulated according to the requirements of the organism. Hierarchical organization and regulation of the hematopoietic populations is preserved in the bone marrow within specific stromal microenvironments named “niches” [43]. Osteoblastic/endosteal niche is composed by mesenchymal stem cells, endosteal fibroblasts and osteoblasts around bone trabeculae. The vascular niche is localized in the inter-trabecular lacunae and includes endothelial and adventitial reticular cells [44]. These virtually-distinct microenvironments and their cellular compositions ensure different functions. According to an oversimplified view, in order to promote self-renewal, osteoblastic niche is involved in quiescent hematopoietic stem cells maintenance while the vascular niche sustains differentiation and mobilization to peripheral circulation of hematopoietic cells [45]. Therefore, the hematopoiesis is closely

related to the features of bone marrow microenvironment, structural (i.e. extracellular matrix proteins), chemotactic (i.e. CXCL12/CXCR4) and adhesion (i.e. E- and P-Selectins) factors gradients [46]. Signals originating in these stromal niches orchestrate hematopoietic cell localization, maturation and mobilization according to the situations.

1.6 Tumor-driven emergency myelopoiesis

In addition to the local modifications, neoplasms exploit the innate and adaptive immune system by inducing a deep and systematic remodelling of the host's myelopoiesis [47]. In response to stimuli, the BM is influenced by the production of hematopoietic cytokines at distant sites that modify physiological myelopoiesis, HSCs expansion and differentiation. Early hematopoiesis is shaped to satisfy increased immune cells demand; it's a "long-distance" regulatory feedback named "emergency myelopoiesis". Emergency myelopoiesis is associated with pronounced increase of cytokines as granulocyte, macrophage and granulocyte-macrophage colony stimulating factors (G-CSF, M-CSF, GM-CSF) and hematopoietic cytokines (SCF, IL-3, IL-6, Flt3 ligand) [48]. Therefore, uncommitted stem cells are instructed to differentiate into myelomonocytic lineage to supply neutrophils and macrophages from the BM. In mice, CMPs generate different subsets of cells identified by cell-surface markers: monocytes ($CD11b^+$ $Gr1^+$ $F4/80^+$), granulocytes ($CD11b^+$ $Gr1^{high}$ $F4/80^-$ $IL\text{-}4R^+$) and MDSCs ($CD11b^+$ $Gr1^{med}$ $F4/80^{low/-}$ $IL\text{-}4R^+$) [49]. Tumor cells recruit monocytes from peripheral blood, thanks to the CCL2 and CCL5 [50] chemokines and contribute to TAM differentiation, whereas circulating neutrophils are driven towards activated tissue neutrophils. Also MDSCs accumulate at tumor sites becoming more suppressive over T cell-mediated immunity [51], promoting tumor development by inducing angiogenesis [52], endothelial to mesenchymal transition (EndoMT) and metastases [53]. Recent studies strongly suggest a correlation between tumor burden and number of tumor-infiltrating MDSC, whose presence is associated with poor diagnosis [54,55]. Perturbed hematopoiesis driven by cancer have been mostly investigated in advanced tumor stages especially in cancer mouse models. However, the mechanisms through which a nascent neoplastic clone send signals to the bone marrow toward the instruction of a

tumor-educated hematopoiesis are unknown. Understanding the phenotypic and molecular determinants of cancer-driven hematopoietic adaptation would offer a new prospect on cancer early detection and prognostication.

1.7 Rationale and Objective

The aim of this three-year study was to investigate the reciprocal interactions between neoplastic cells and the surrounding stromal microenvironment. We challenged the hypothesis that stromal and immunological components actively control the transition from pre-malignant lesions to cancer.

In particular, we focused on two specific areas of interest: tumor micro- and macroenviromnent and how these systems affect tumor establishment and progression. First we investigated the contribution of local MCs to tumor progression and differentiation, and the therapeutic effects of Imatinib tyrosine kinase inhibitor on MCs in the spontaneous prostate cancer TRAMP model [56]. This transgenic mouse also allowed us to examine the immunosuppressive features of MCs in promoting immune tolerance and modifying tumor phenotype. In the second part of the study, postulating that cancer-associated immunosuppression involves hematopoietic reprogramming, we investigated systemic modifications occurring in the BM hematopoietic microenvironment at discrete stages of tumor development, from pre-malignant to invasive stages. To carry on this idea, spontaneous MMTV-NeuT model of mammary cancerogenesis [57] was used. The integration of histopathological and immunophenotypical analyses and quantitative *in situ* immunolocalization analyses offered a new insight into the involvement of micro- and macroenvironment in tumor progression and clinical outcome.

CHAPTER 2

Materials and Methods

2.1 Mice and treatments

Animals were maintained in filter-top cages at the Fondazione IRCCS Istituto Nazionale Tumori in Milan. All procedures involving animals were carried out under pathogen-free conditions and performed in accordance to the institutional guidelines and national law (D.lgs 26/2014).

A spontaneous model of prostate cancer (TRAMP) on C57BL/6J background, which express SV40 small and large T antigens under the control of the androgen-driven rat probasin regulatory element [56] were used. Mice deficient in mast cells (Kit^{Wsh}-TRAMP) were generated by crossing TRAMP mice with MC-deficient Kit^{Wsh} [58]. $CD40^{-/-}$ mice were obtained thanks to the collaboration with San Raffaele Scientific Institute in Milan). Imatinib (50mg/kg) was inoculated intraperitoneum 5 times a week from 8 to 25 weeks.

For T-cell depletion experiments, the thymus of 16-week-old TRAMP and Kit^{Wsh}-TRAMP mice was surgically removed. The following day, mice were treated i.p. with 300 μg of depleting antibodies to CD4 and CD8 of age. Mice were sacrificed at 25 weeks and their urogenital apparatus collected for IHC.

BALB-NeuT female mice expressing the transforming rat oncogene c-erbB2 (Her2/neu) under the mouse mammary tumor virus (MMTV) promoter spontaneously develop mammary carcinoma with a well-defined tumor progression [57,59] .Female

NeuT- (BALB/c) mice were crossed with male NeuT+ mice and positive female were monitored weekly for mammary tumor development and progression.
Separate groups of mice were sacrificed at different phases of disease progression, 6 and 12 weeks of age, time points that reflect early stages in which tumor is not palpable yet and at 24 weeks of age when the tumor is visible. Mice were sacrificed, femurs and mammary glands were collected.

2.2 Mice reconstitution with bone marrow-derived mast cells (BMMC)

Bone marrow precursors from C57BL6/J or CD40L$^{-/-}$ mice were cultured *in vitro* in RPMI with 20% FBS, and 20 ng/mL both SCF and IL3 [60]. After 4 weeks, when purity was more than 90% 5x10^6 BMMCs were injected i.p. into 8-week-old mice.

2.3 Histopathology and immunolocalization analyses

Human primary tumor samples were obtained from the pathology archives of the Human Pathology Section, Department of Health Sciences (University of Palermo, Italy). Human tumor specimens, murine urogenital apparatus, bone marrow and mammary gland samples were fixed with 10% neutral buffered formalin overnight, washed in water, decalcified (BM samples only) and then paraffin embedded. Subsequently, four-micrometers-thick sections were cut and used for both histopathology (hematoxylin & eosin) and immunostainings.
For evaluation of MC infiltration, prostate sections were stained with toluidine blue.
Immunohistochemistry (IHC) was performed using a horseradish peroxidase (HRP) and Alkaline phosphate (AP) methods. The antigen unmasking technique was performed using Novocastra Epitope Retrieval Solutions pH9, pH8 and pH6 in PT Link Dako at 98°C for 30 minutes. Subsequently, the sections were brought to room temperature and washed in PBS. After neutralization of the endogenous peroxidase with 3% H_2O_2 and Fc blocking by a specific protein block the samples were incubated overnight at 4 C° with the following primary antibodies: Rabbit polyclonal CK8 (1:100 pH9; Abcam), Rabbit Polyclonal c-Kit (1:50 pH6; Acris); Rabbit Polyclonal Ki67

(1:1000 pH6; Abcam); Rabbit Polyclonal CD40L (1:250 pH6; Abcam); Mouse Monoclonal CD33 (Clone PWS44; 1:100 pH9; Leica Biosystems); Mouse Monoclonal Mast Cell Tryptase (Clone 10D1; 1:150; Leica Biosystems); Mouse Monoclonal CXCL12/SDF-1(Clone #79018; 1:50 pH6; R&D Systems); Rabbit Monoclonal CXCR4 (Clone UMB2; 1:100 pH6; Epitomics); Mouse Monoclonal Nestin (Clone rat-401; 1:100 pH9; Millipore); Rabbit Polyclonal ATF3 Activating transcription factor 3 (1:50 pH8; Sigma-Aldrich); Rabbit polyclonal Myeloperoxidase (1:25 pH9; Abcam), Rat monoclonal Ly76 (Clone TER-119; 1:50 pH9; Abcam), Rabbit monoclonal Pax5 (Clone EPR3730(2); 1:1000 pH9; Abcam). Staining was revealed using IgG (H&L) specific secondary antibodies (Life Technologies, 1:500) or SuperSensitive Link-Label IHC Detection System Alkaline Phosphatase (Biogenex).

AEC (3-Amino-9-Ethylcarbazole), DAB (3-3' diaminobenzidine) and Vulcan Fast Red were used as substrate chromogen. The slides were counterstained with Harris hematoxylin (Novocastra). For CXCR4/CXCL12 double-marker immunofluorescence, two sequential rounds of immunostaining were performed using Alexa-568- and Alexa-488-conjugated specific secondary antibodies (Life Technologies). For triple immunofluorescence stainings, tissue samples were incubated with the following primary antibodies: FITC- anti mouse Gr1, APC- anti mouse CD3, (both from eBiosciences), and anti mouse triptase (AbCam, Cambridge, UK) followed by rat- anti mouse alexa 546 (Invitrogen). Alternatively anti mouse CD40 (eBiosciences) followed by rat- anti mouse alexa 488 (Invitrogen), anti mouse triptase (AbCam, Cambridge, UK) followed by rat- anti mouse alexa 546 (Invitrogen) and APC- anti mouse Gr1 (eBiosciences) were used.

All the sections were analysed under a Zeiss AXIO Scope.A1 microscope (Zeiss, Germany) and microphotographs were collected using a Zeiss Axiocam 503 Color digital camera using the Zen2 imaging software.

2.4 Disease score and tumor burden

Disease score and tumor burden of prostate and mammary lesions were evaluated on H&E-stained sections. Prostates lesions of TRAMP mice were scored as hyperplasia or intraepithelial neoplasia (HYP-PIN), adenocarcinoma (ADENO) and

neuroendocrine tumor (NE). For determination of the mammary gland disease score, the extension (focal, 1; multifocal, 2; diffuse, 3) and severity (mild, 1; moderate, 2; severe, 3) of hyperplasia and dysplasia, the extension of in situ or infiltrating carcinoma foci, the extension and severity of stromal remodelling, and the severity of inflammatory infiltrate were scored according to a combined semi-quantitative score. The overall disease score was calculated as the sum of the individual variables scores. For tumor burden calculation, three non overlapping panoramic microphotographs (at 5x magnification) were collected from each sample and analyzed using the Zen 2.0 software (Zeiss), by contouring the foci of high-grade dysplasia/PIN, *in situ* carcinoma, and invasive carcinoma, and quantifying the extension of the relative areas (μm^2).

2.5 Quantification of spatial relationship in bone marrow tissue samples

Quantitative immunolocalization analyses were performed using an *ad-hoc* developed software coded in Python language (Oliphant TE, Computing in Science and Engineering 2007), which, after a process of segmentation of microphotographs, evaluated the distances between IHC-labeled regions and selected regions of interest. Specifically, IHC-labeled cells and extracellular structures, along with nuclei were automatically segmented while vessels and bone trabeculae were morphologically identified and selected by an expert pathologist (C.T.). The software calculated the number of pixels of the segmented IHC-labeled areas, and the minimum distance of each pixel from the selected regions of interest, creating a graph of distance distribution. Differences in the distance distribution of IHC markers from the selected regions of interest were calculated according to the Kolmogorov-Smirnov test. Two distributions were considered different for p-values <0.01.

CHAPTER 3

Results

3.1 Mast cells protect against neuroendocrine tumor development

Transgenic adenocarcinoma prostate mouse (TRAMP) model progressively develops hyperplasia or intraepithelial neoplasia (HYP-PIN) at 8-16 weeks, *in situ* adenocarcinoma (ADENO) at 16-24 weeks and eventually metastasis [61], mimicking the human disease. As in human, prostate tumors can also evolve in poorly differentiated neuroendocrine phenotype (NE) in about 15-20% of TRAMP mice [62] .

In this context, in a cohort of 25-week-old-mice we evaluated prostate tumor histology on H&E-stained sections (Fig. 1a) and scored the lesions as adenocarcinomas when stromal invasion by atypical cells expressing cytokeratin 8 (CK8) (Fig. 1a) was observed. Ki-67 immunostaining highlighted the different proliferation of TRAMP adenocarcinomas and NE tumors. In particular NE tumors showed a higher fraction of proliferating malignant elements in comparison with adenocarcinomas (Fig. 1b).

According to our previous data [60] , tumor-infiltrating MCs showed strong positivity for cKit staining among negative adenocarcinomas cells, whereas NE tumor cells diffusely showed a mild positivity for cKit (Fig. 2a). The results obtained in the mouse model were also confirmed in human prostate cancers (Fig. 2b).

Prompted by the concomitant expression of c-Kit on MCs, NE tumor cells and the prostate stem cells (PSCs) compartment [63], we investigated the role of the mast cells in the TRAMP model.

To evaluate whether the adenocarcinoma progression was altered by the absence of MCs, Kit^{Wsh}-TRAMP were generated by crossing TRAMP mice with MC-deficient Kit^{Wsh} mice [58]. H&E staining showed multifocal infiltrating prostate adenocarcinoma in TRAMP mice (80%) whereas a minor fraction developed NECs (13%) and only few had dysplasia or prostatic intraepithelial neoplasia (PIN; 7%). Conversely, Kit^{Wsh}-TRAMP mice showed impaired adenocarcinoma growth (21.4%), but a larger portion of the mice showed only dysplastic foci or intraepithelial neoplasia and an increased frequency of NECs (42.9%) (Fig. 3). These data revealed a marked propensity in Kit^{Wsh}-TRAMP mice to a NE transformation, suggesting a protective role of mast cells against malignant neuroendocrine differentiation.

3.2 Imatinib treatment restrains growth of adenocarcinoma but not of neuroendocrine prostate tumors

In light of the common expression of c-Kit on MCs infiltrating ACs and NE tumor cells[63], we hypothesize that cKit inhibition could impair both adenocarcinoma-promoting MCs activity and NE tumor cell growth. Therefore, we investigated that Imatinib mesylate, a drug-targeting cKit, should be able of eliminating both adenocarcinoma, via MCs inhibition, and the NE variants, via direct effect on NE tumor cell. Imatinib is a well-known tyrosine kinase inhibitor, currently approved for the treatment of chronic myelogenous leukemia [64], and gastrointestinal stromal tumors [65], which targets the intracellular ABL kinase and the fusion oncogene BCR-ABL of chronic myeloid leukemia [66] and the surface receptors cKit and PDGFRs [67].

TRAMP mice were treated with Imatinib from 8 to 25 weeks of age and the urogenital apparatus was collected for histopathological analyses. The treatment significantly reduced the incidence of adenocarcinomas by neutralizing mast cell activity (47.1% vs 76,9% of untreated TRAMP mice), but had no effect against NE tumors which were significantly increased (23.5% vs 15.4% of untreated TRAMP mice (Fig. 4a). The expression of c-Kit was maintained in NE tumors treated with Imatinib (Fig. 4b), which ruled out that loss of receptor expression could underlie Imatinib resistance.

Evaluations of toluidine blue-stained sections in untreated TRAMP mice showed accumulation and degranulation of MCs preferentially around PIN and well differentiated ACs areas, while MCs were absent in NE (Fig. 5a,b). Imatinib treatment

did not affect the average of MCs density nor their degranulation status (Fig. 5c). We did not find appreciable differences in the inflammatory infiltrates of TRAMP and Kit^{Wsh}-TRAMP mice, which usually showed moderate mixed inflammatory infiltrates rich in neutrophils and eosinophils. In contrast, Imatinib-treated mice showed poor peritumoral inflammation with a prevalence of lymphocytes.

These data suggested that Imatinib treatment alters cross-talk between prostate transforming cells and mast cells, promoting adenocarcinomas suppression but, unexpectedly, increasing NE variants insensitive to Imatinib treatment despite expressing cKit.

3.3 Addition of mast cells restored CD8+ T-cell unresponsiveness and tumor growth

After confirming the mast cell contribution to adenocarcinoma onset and progression, we assessed whether this observation was related to their immunosuppressive capacity. We investigated whether mast cells promote tolerance to SV40 Large-T-antigen, the transforming oncogene in TRAMP mice. To prove the involvement of mast cells in supporting prostate adenocarcinoma growth, we reconstituted Kit^{Wsh}-TRAMP mice with bone marrow-derived mast cells (BMMC). Histological sections of prostate stained with toluidine blue and relative quantification showed correct repopulation and distribution of mast cells in recostituited Kit^{Wsh}-TRAMP (Fig. 6a,b). Prostatic lesions H&E-evaluated, highlighted 60% of Kit^{Wsh}-TRAMP mice reconstituted with BMMCs developed adenocarcinomas, whereas only 21.4% of nonreconstituted mice developed adenocarcinomas (Fig. 6c). To further confirm that mast cells restored $CD8^+$ T-cell unresponsiveness and tumor growth, we depleted *in vivo* both $CD4^+$ and $CD8^+$ T lymphocytes by surgical removal thymus, followed by administration of specific depleting antibodies and analysed prostate histology. In T cell-depleted Kit^{Wsh}-TRAMP, the frequency of infiltrating adenocarcinoma increase reaching comparable levels with TRAMP mice (Fig. 7a,b). On the contrary, adenocarcinoma growth was unaltered in TRAMP mice regardless of whether or not T cells were depleted (Fig. 7a,b). This result is consistent with the unresponsiveness of tumor-specific T cells in

these mice. Thus, mast cells impair tumor-specific $CD8^+$ T cell activity, allowing adenocarcinoma growth in TRAMP mice.

3.4 Mast cell CD40L triggered PMN-MDSC CD40 to suppress T-cell function

The obtained results indicate that mast cells can hamper tumor-specific $CD8^+$ T-cell responses through either direct or indirect interaction between mast cells and T cells. Immunofluorescence analyses revealed that in the spleen of TRAMP mice, mast cells are not present in the splenic white pulp and do not colocalize with CD3-expressing cells. On the contrary we found mast cells within the splenic red pulp, in close contact with $Gr1^{hi}$ cells (Fig. 8). Gr1 antibodies identify MDSCs recognizing both Ly6C and Ly6G epitopes [68]. Therefore, mast cells can enhance MDSCs suppressive activity through direct interaction [31,69]. We investigated the mechanism used by mast cells to enhance PMN-MDSC suppression.

Recent findings suggested that CD40 is already associated to MDSC suppression[70]. CD40L expression on BM-derived mast cells cultured *in vitro* was confirmed by our collaborators in Milan. The colocalization between mast cells and CD40 in the spleen was visualized by triple immunofluorescence with Gr1, CD40 and the mast cell-marker Tryptase (Fig. 9a). To further confirm the role of the CD40L-CD40 axis in the interaction between mast cells and PMN-MDSCs, we reconstituted Kit^{Wsh}-TRAMP mice with BMMCs obtained from either wild-type or $CD40L^{-/-}$ mice and analysed prostate lesions. Adenocarcinoma burden, expressed in μm^2, in Kit^{Wsh}-TRAMP mice reconstituted with $CD40L^{-/-}$ BMMCs was significantly reduced (17.2% *in situ* and 10.3% infiltrating adenocarcinoma on total tumor burden, respectively) in comparison to TRAMP (17.2% *in situ* and 78.5% infiltrating adenocarcinoma) and Kit^{Wsh}-TRAMP mice reconstituted with wild-type BMMCs (28.1% *in situ* and 57.2% infiltrating adenocarcinoma), and it was even lower in comparison to unreconstituted Kit^{Wsh}-TRAMP (40.36% *in situ* and 30.11% infiltrating adenocarcinoma) (Fig. 9b,c). These results indicate that expression of CD40L on mast cells supports their cross-talk with PMN-MDSC, favouring immune escape and adenocarcinoma development.

Quite the opposite, the absence of CD40L prevents the MC/MDSC cross-talk, restores anti-tumor T-cell response and decreases consequently adenocarcinomas development. We have previously shown that in human prostate cancer, mast cells accumulate in well-differentiated tumors more than in poorly differentiated areas [60]. Immunohistochemistry on serial sections of human prostate cancer samples highlighted the presence of cells positive for tryptase, CD40L and CD33 used as a myeloid cell marker (Fig. 10a) in well-differentiated areas. Immunofluorescence confirmed coexpression of tryptase and CD40L on tumor infiltrating mast cells, and proximity of mast cells to $CD33^{+}$ cells (Fig. 10b,c).

3.5 Bone marrow hematopoietic alterations at infiltrative stage of peripheral mammary cancerogenesis

Following the demonstration that the presence and activation status of myeloid elements within the local microenvironment of spontaneous tumors could impact its phenotypic outcome, I focused on the general mechanisms that could be responsible for reprogramming the myeloid cell output under the pressure of malignant transformation. Transgenic NeuT+ mice represent a powerful tool for studying all stages of breast cancer development and progression. We investigated BM hematopoietic changes in term of cell number and spatial organization at defined stage of mammary primary lesion. The histopathological and immunolocalization analyses was performed at three different time points, 6, 12 and 24 weeks of age that reflect early stages in which tumor is not palpable, pre-invasive and invasive stages. The simultaneous morphological analysis of peripheral mammary lesions (dysplasia, *in situ* carcinoma, invasive carcinoma) and bone marrow specimens allowed to correlate neoplastic clone development and adaptation of hematopoietic response. For each mouse of our cohort the histopathological characterization of primary lesions was performed on routinely-stained H&E sections and the stage of disease progression scored. As comparison, control BALB/c (NeuT) mice were analyzed (Fig. 11a). The overall disease severity score was calculated as a sum of the extension (focal, 1; multifocal, 2; diffuse, 3) and severity (mild, 1; moderate, 2; severe, 3) of hyperplasia and dysplasia, the extension of *in situ* or infiltrating carcinoma foci, the extension and

severity of stromal remodelling and of inflammatory infiltrate (Fig. 11b,c). Histochemical analysis showed a profound modification in the hematopoietic BM during advanced tumor progression stage. Specifically, the BM parenchyma of 24w NeuT+ mice showed a marked granulocytic myeloid hyperplasia, which was characterized by a prominent enrichment in morphologically immature granulocytic elements and associated with a contraction of erythroid precursors and lymphoid elements. These features were absent in the BALB/c bone marrow (Fig. 12a). No significant differences were observed in the density and morphology of megakaryocytes. In order to confirm the modifications observed in hematopoietic cell populations H&E-stained, immunolocalization analyses are performed. Immunohistochemical stainings confirmed the increase of the density of myeloid cells, also including hyposegmented immature forms, highlighted by myeloperoxidase (MPO), the detriment of erithroid elements identified by Ter-119 and of B cells pools detected by PAX5 marker (Fig. 12b). The differences between NeuT and BALB/c hematopoietic bone marrow are quantified, confirming histochemical and immunohistochemical evaluations (Fig. 12c). These data suggest that an advanced-stage peripheral neoplasia supports an altered hematopoiesis in the bone marrow.

3.6 Bone marrow hematopoietic adaptation is identified at pre-invasive and pre-malignant stages

Starting from this evidence, we moved to earlier time point, specifically pre-invasive or pre-malignant stages, to test whether signs of BM modifications could be detected. Also hematopoietic marrow of 12 weeks old NeuT+ mice, corresponding to *in situ* carcinoma, showed a clear expansion of granulocytic myeloid cells and depression of lymphoid and erythroid elements, as compared with BALB/c controls (Figure 13a). The same alterations, though less prominent, were also highlighted in the bone marrow of 6 weeks NeuT+ mice (Fig. 13b), in which the mammary glands present a pre-cancerous stage with a moderate-to-severe epithelia dysplasia.
In both groups hematopoietic changes were quantified (Fig. 13 c,d).

Consistently with our hypothesis, most of the differences that were significant at 24 weeks, were also identified in 12 and 6 weeks BM samples, proving that an incipient neoplasia influences the bone marrow by activating hemopoiesis tumor-adapted.

3.7 Bone marrow stromal architecture alterations at early stages of peripheral cancerogenesis

In order to determine the functional relationship between hematopoietic components and mesenchymal stromal compartment during altered bone marrow homeostasis, we deepened the changes in the BM stromal architecture. Through *in situ* immunolocalization analyses, we could also demonstrate that mesenchymal cells, which amount for less than 5% of whole BM cellularity, underwent significant modification in their density and localization already at 12 and 6 weeks. Indeed, Nestin+ BM mesenchymal stromal elements expanded in the BM ostoblastic (precursor-rich) and vascular (mature-cell-rich) niches and showed consistent upregulation of the prototypical chemotactic stromal CXCL12 in transgenic mice as compared with control mice (Fig. 14 a,b,d).

Indeed, while in the hematopoietic lacunae of BALB/c mice Nestin+ and CXCL12 was mostly confined to the vascular area, in NeuT+ mice, the expression of Nestin and CXCL12 was more prominent in the peri-vascular and interstitial area. Such modifications were quantified by an *ad-hoc* software analysis applied to immunostained BM sections thanks a collaboration with Dr. Maurizio Marrale of the University of Palermo (Fig. 15). This software was applied to the vessel proximity distribution of Nestin- and CXCL12-expressing cells in BALB/c and NeuT mice. This novel tool for automated image software analysis allowed to reproducibly quantified spatial modification of different BM elements (Fig. 15).

The relocalization of Nestin+ meshwork and CXCL12 expression suggested an alteration in the hematopoietic niche. Consistent with these changes, in BM was also an overall expression of the CXCL12 chemotactic receptor CXCR4, which was significantly increased in myeloid cells of 6 and 12 weeks NeuT+ mice (Fig. 14 c,d)

The co-occurrence of CXCL12/CXCR4 induction in the same hematopoietic environment was confirmed by double marker immunofluorescence analysis on 12 weeks BM samples. The double staining showed the coherent modulation of CXCL12 and CXCR4 in the hematopoietic interstitium (Fig. 16).

Overall these results highlighted that the early modifications occurring in the BM parenchyma at premalignant phases of cancer development, mainly concern an innate immune cell subset, specifically granulocytic myeloid cells, that are enriched at the expenses of other resident populations being favoured in their repositioning within BM erythroid and lymphoid niches by the CXCL12/CXCR4 axis.

These BM alterations could represent a crucial mechanism for defining the bone marrow an early sensor of neoplastic transformation.

CHAPTER 4

Concluding Remarks

Overall, the experimental effort of my PhD program, which is summarized in the present thesis, allowed identifying new micro- and macro-environment dynamics relevant to the outcome of malignant transformation in two spontanous models of cancerogenesis recapitulating the transforming stages of two highly prevalent malignancies. I could demonstrate that mast cells recruited at foci of malignant epithelial transformation towards prostate adenocarcinoma exert immune suppressive functions favoring cancerogenesis, but at the same time allow transforming cells to maintain their glandular differentiation preventing the outburst of anaplastic tumors with neuroendocrine features. Besides consolidatign and applying my knowledge of in situ investigation methods I could develop a mechanistic view of the observed phenotype and challenge the relevance of a molecular axis based on CD40- and CD117-mediated signals. The increasing amount of evidence regarding the plethora of functions played by different types of hematopoietic cells within the tumor microenvironment represented a strong motivation towards my involvement in investigating the tumor environment from a systemic perspective, focusing on the hypothesis that perturbation of the innate and adaptive immune cell functions could be traced back to the hematopoietic process. The finding of measureable hematopoietic alterations occurring at the pre-malignant stages of peripheral malignant transformation was an exciting discovery which changed my view of tumor-associated immune impairment from a local event to a systemic disease. Indeed, cancer is commonly regarded as a systemic disease only when in a metastatic stage, yet its influence over

systemic homeostatic processes such as hematopoiesis, adipose tissue metabolism, microbiota regulation may characterize the earliest stages of its development. The results of my effort within the frame of the research units led by Professor Tripodo (Tumor Immunology Unit, University of Palermo) and by Dr Mario Paolo Colombo (Molecular Immunology Unit, National Cancer Institute, Milan) will constitute the bases for my future activity in cancer research.

CHAPTER 5

Figures and Tables

5.1 Mast cells protect against neuroendocrine tumor development

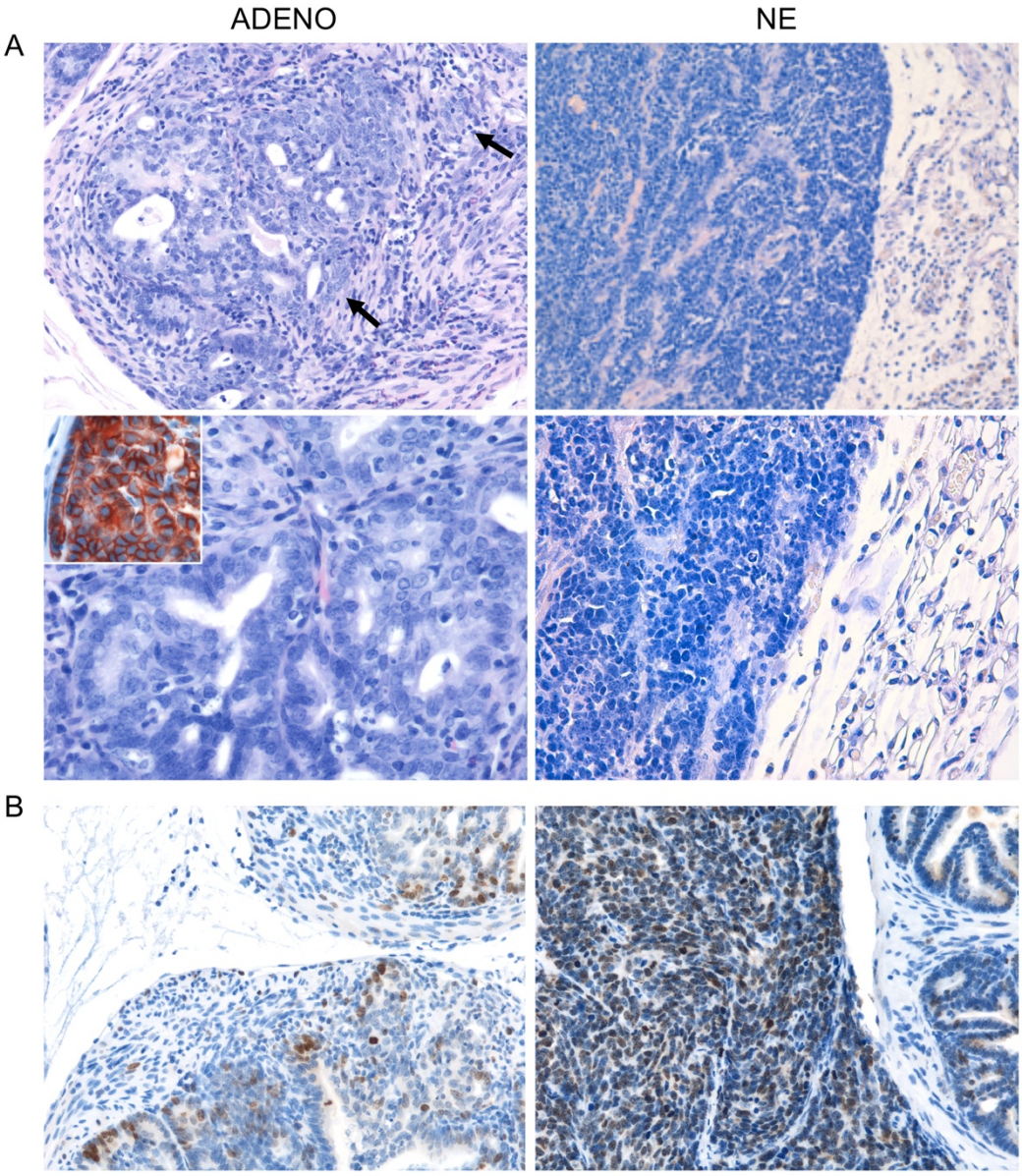

Figure 1: (a) Representative H&E staining of prostates of 25 weeks old TRAMP mice showing evidence of infiltrating adenocarcinoma (ADENO; left panel) or NE tumor (right panel). Arrows indicates areas of stromal invasion. Magnification 20x or 40X in upper or lower panels, respectively. Inset in lower left panel: CK8 staining (in red) in TRAMP adenocarcinoma highlighting areas of stromal invasion of tumor epithelial cells. Magnification 40x. **(b)** Representative Ki-67 staining (in brown) of prostates of 25 weeks old TRAMP mice showing evidence of infiltrating adenocarcinoma (ADENO; left panel) or NE tumor (right panel). Magnification 20x.

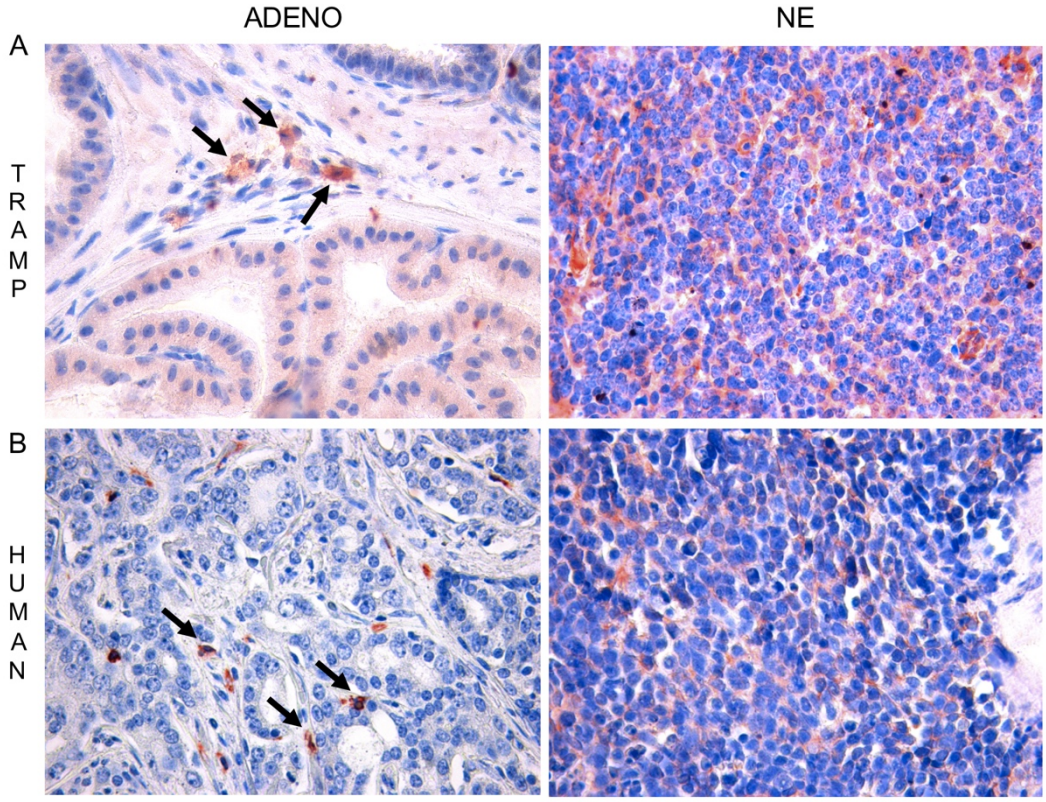

Figure 2: (a,b) Representative cKit staining of prostates of 25-week-old TRAMP mice (a) or human patients (b) bearing adenocarcinoma (ADENO; left) or NE tumors (right). Magnification 40x. Arrows indicate cKit-positive MCs within adenocarcinoma.

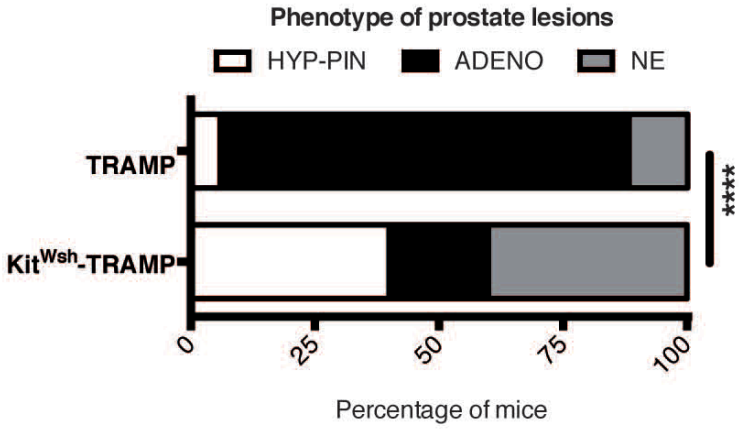

Figure 3: Graph depicts the relative percentage of dysplasia/PIN, adenocarcinoma (ADENO) or neuroendocrine (NE) lesions in 25-week-old TRAMP (n=17) and KitWsh-TRAMP mice (n=15). Fisher test: ****, $P < 0.0001$.

5.2 Imatinib treatment restrains growth of adenocarcinoma but not of neuroendocrine prostate tumors

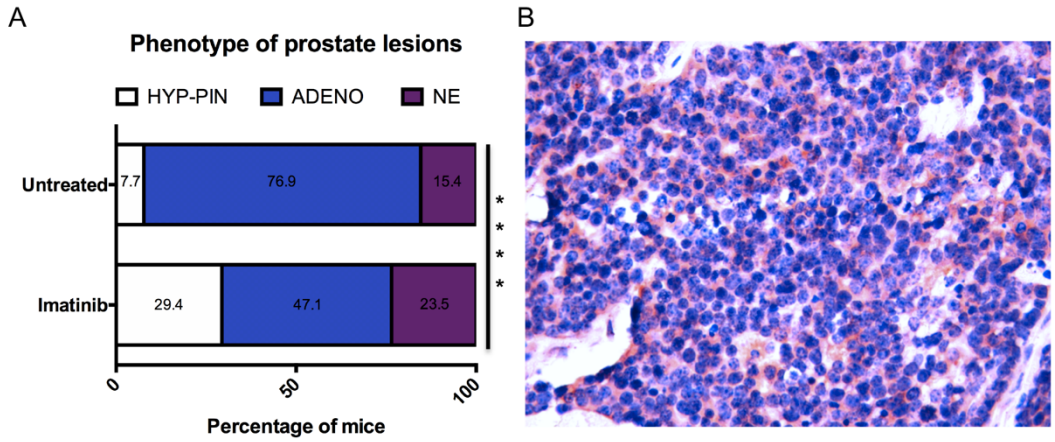

Figure 4: (a) TRAMP mice were either left untreated (n=13) or treated from 8 to 25 weeks of age with imatinib (n=17). Graph depicts the relative percentage of lesions scored as hyperplasia-prostatic intraepithelial neoplasia (HYP-PIN, white area), adenocarcinoma (ADENO, light blue area), or neuroendocrine (NE, violet area). Numbers within bar represent relative percentages. **(b)** Representative cKit staining of NE tumors grown in TRAMP mice treated with Imatinib. Magnification 40x. Fisher test: ****, $P < 0.0001$.

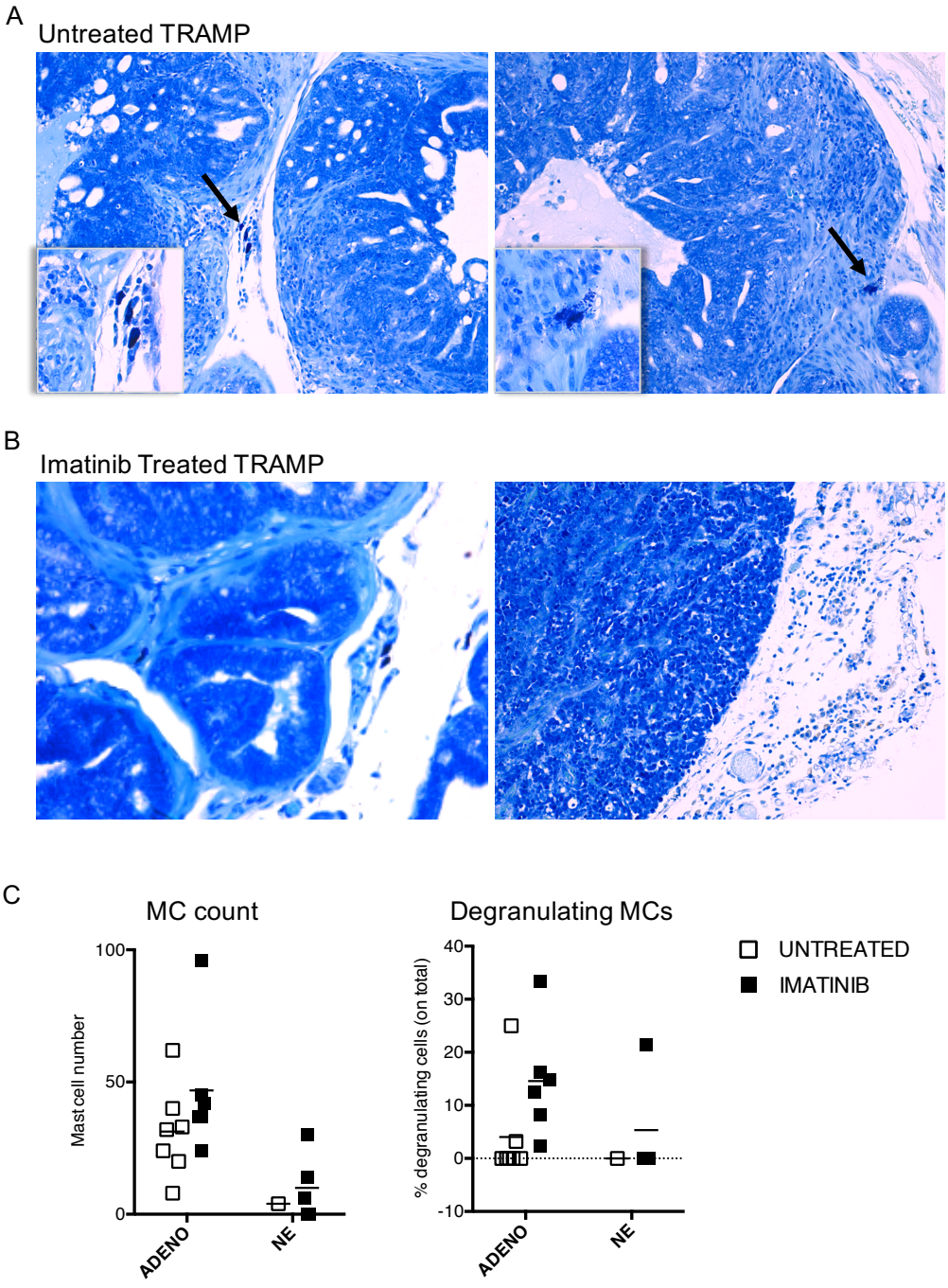

Figure 5: (a,b) Representative toluidine blue staining of prostate of 25 weeks old TRAMP mice either untreated or treated with Imatinib. Arrow highlight MCs. Magnification 20x or 40x. **(c)** Graphs depict the MCs number and degranutation status.

5.3 Addition of mast cells restored CD8+ T-cell unresponsiveness and tumor growth

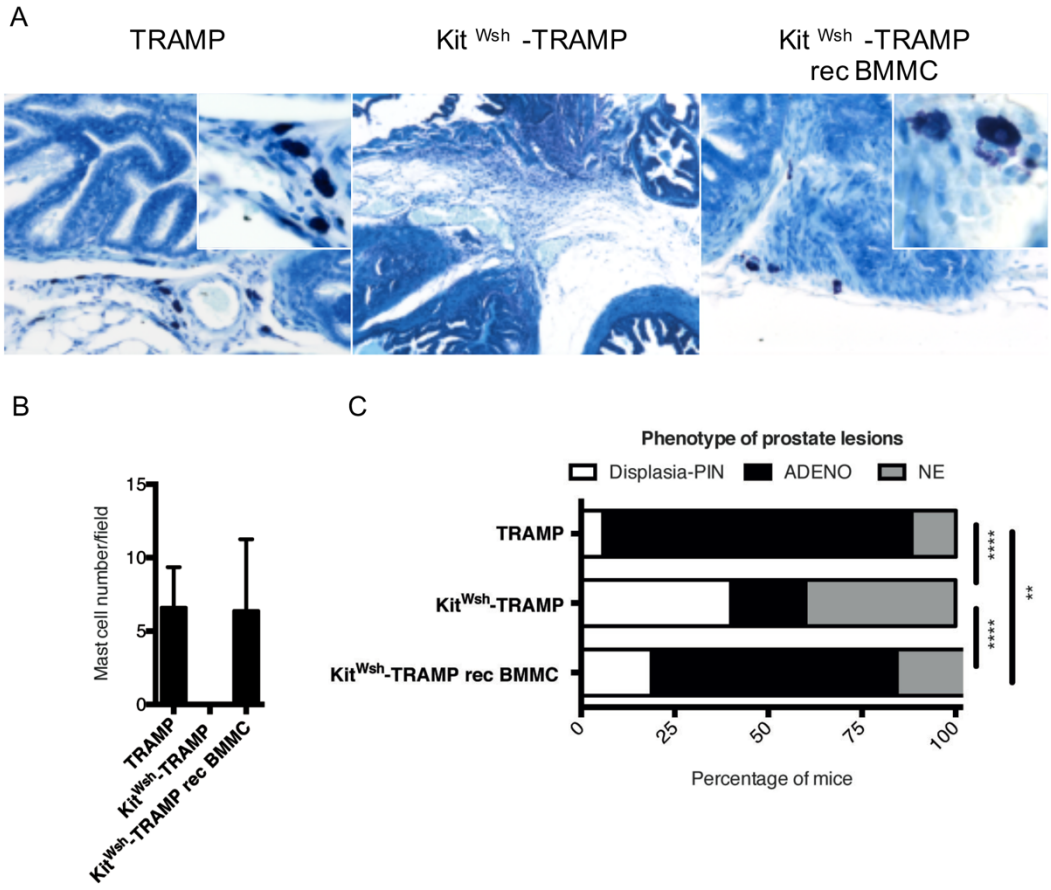

Figure 6: (a) Toluidine blue staining on prostate sections verified reconstitution. Magnification, 20x; insets 40x. **(b)** Quantification of MCs infiltrating prostates of TRAMP, Kit^{Wsh}-TRAMP and reconstituted (rec) Kit^{Wsh}-TRAMP mice was performed on toluidine blue stained sections. MCs counts reported are an average of the count preformed in 5 fields per section.
(c) Evaluation of prostatic lesions of reconstituted KitWsh-TRAMP mice (n=14) killed at 25 weeks, scored as dysplasia/PIN, adenocarcinoma (ADENO), or neuroendocrine (NE). Evaluation of frequency of prostate lesion within each group. Fisher test: **, $P < 0.01$; ****, $P < 0.0001$.

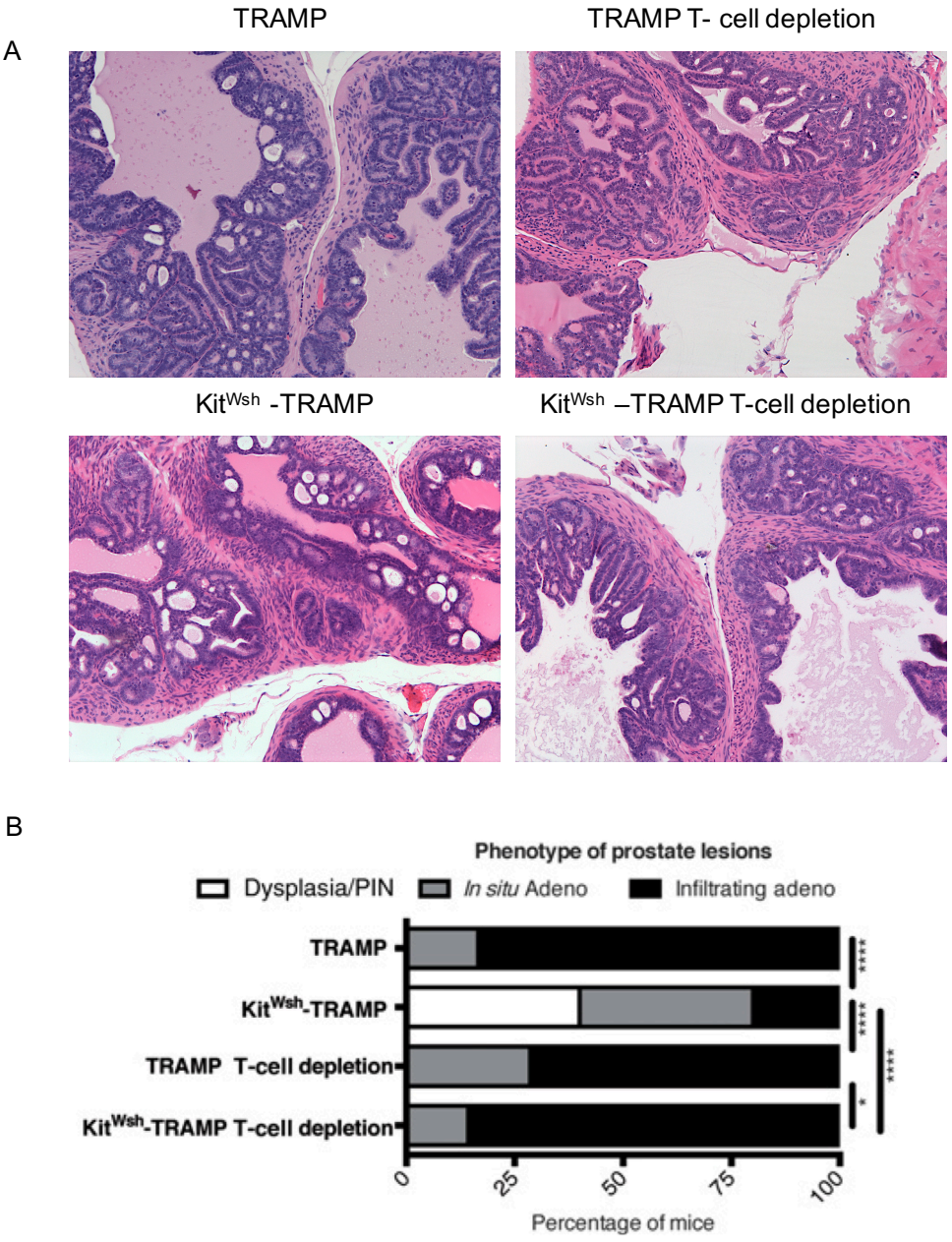

Figure 7: (a) TRAMP and KitWsh-TRAMP (n=6 each group, pooled from two independent experiments) were depleted of T cells when 16 weeks old by surgical removal of thymus and subsequent administration of depleting anti-CD4 and anti-CD8. Treated and control untreated mice were killed at 25 weeks of age, and prostates scored as dysplasia/PIN, in situ ADENO or infiltrating ADENO. Representative H&E staining, magnification 20x. **(b)** Evaluation of frequency of prostate lesion within each group. Fisher test: *, $P < 0.01$; ****, $P < 0.0001$.

5.4 Mast cell CD40L triggered PMN-MDSC CD40 to suppress T-cell function

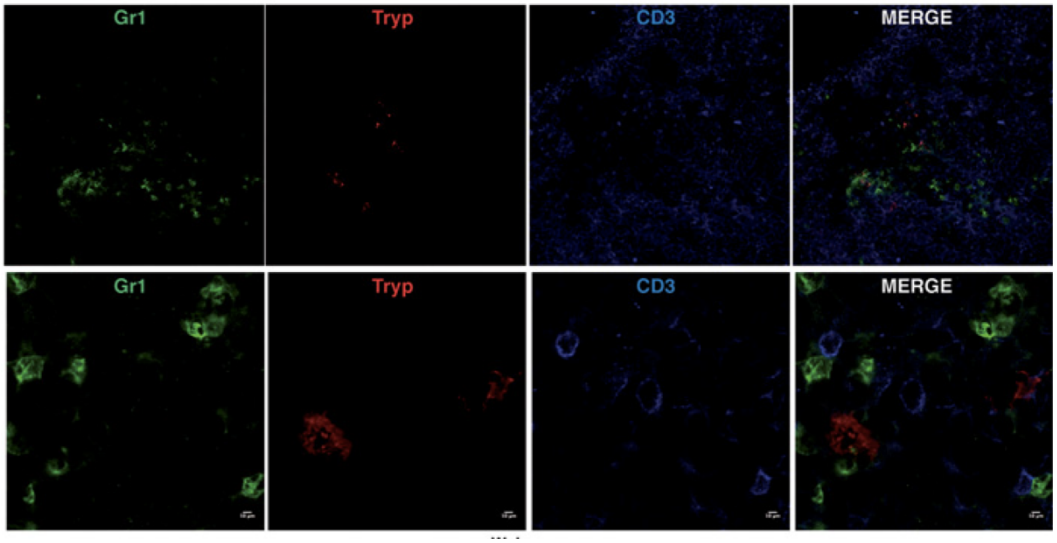

Figure 8: Representative immunofluorescence staining of spleens of 16-week-old TRAMP mice and of control 16-week-old KitWsh-TRAMP mice (magnification 63x). Green: Gr1, red: Triptase, blue: CD3.

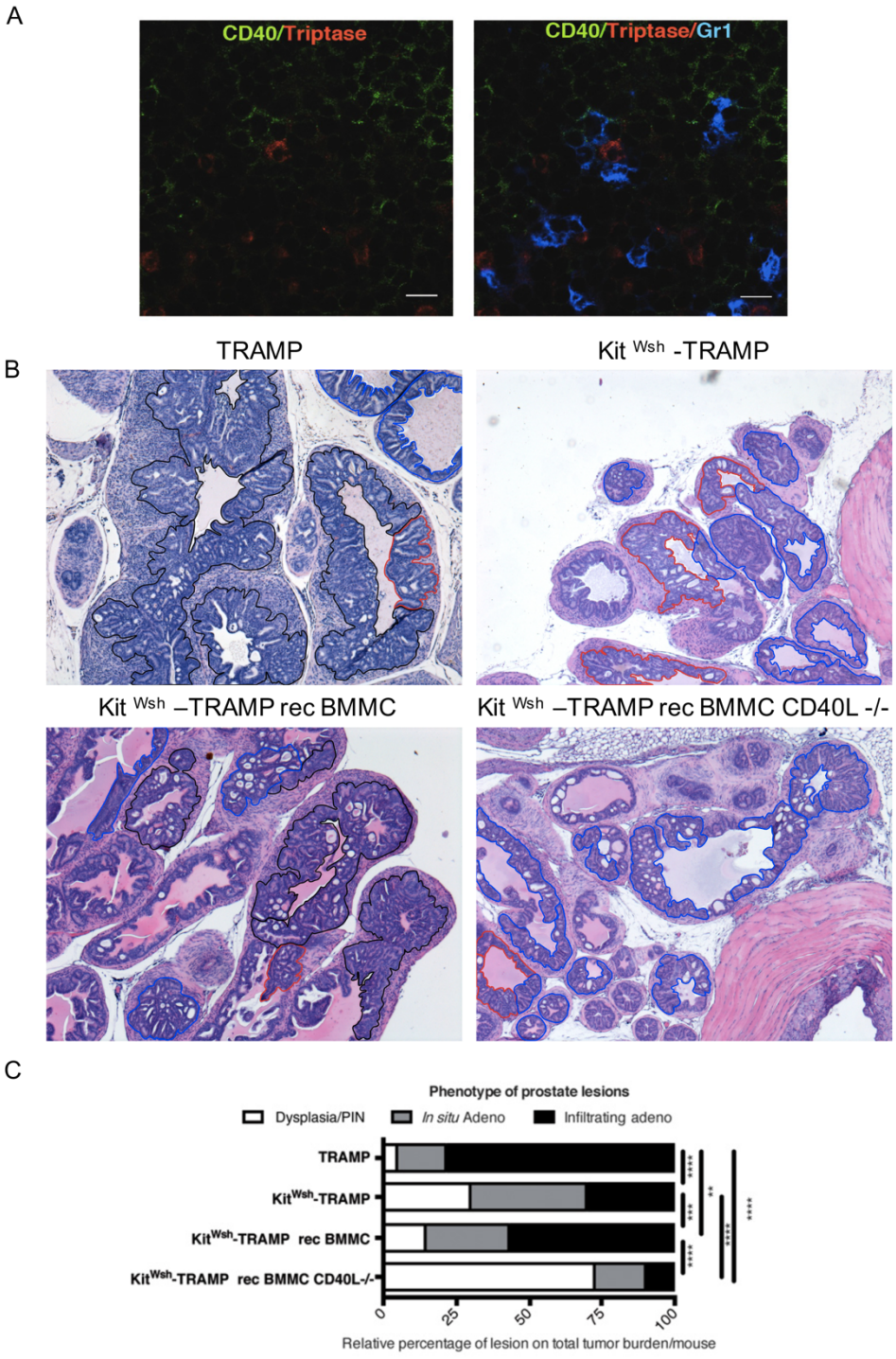

Figure 9: (a) Representative immunofluorescence staining of spleens of 16-week- old TRAMP mice. Green: CD40, red: Triptase, blue: Gr1. **(b)** Mice (n=4 for each group) were killed at 25 weeks of age. Prostates were evaluated for quantitation of areas of dysplasia/ PIN (contoured in blue), in situ adenocarcinoma (contoured in red) or infiltrating adenocarcinoma (contoured in black). Magnification, 5x. **(c)** Graph depicts the relative percentage of each lesion on total tumor burden for each mouse. Experiment was repeated twice. Fisher test: **, $P < 0.01$; ***, $P < 0.001$; ****, $P < 0.0001$.

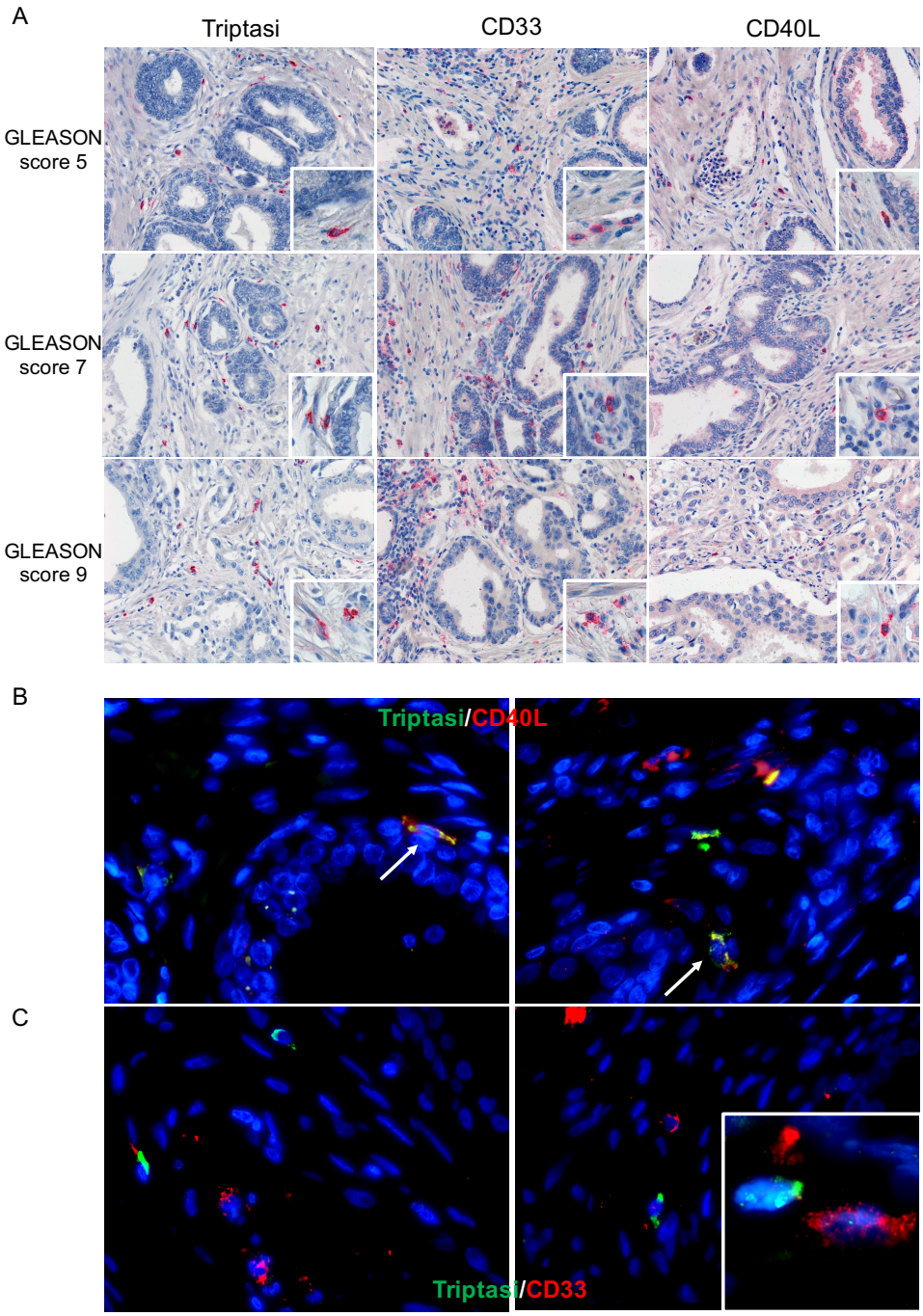

Figure 10: (a) Immunohistochemistry for Triptase, CD40L or CD33 on serial section of human prostate cancer samples representative of different stages (Gleason Score 5, 7 or 9). Magnification 20X, insets 40x. B) Representative immunofluorescence staining on the same human prostate cancer samples. Green: Tryptase, red: CD40L, blue: DAPI. Magnification 63X. C) Representative immunofluorescence staining on the same same human prostate cancer samples. Green: Tryptase, red: CD33, blue: DAPI. Magnification 63X.

5.5 Bone marrow hematopoietic alterations at infiltrative stage of peripheral mammary cancerogenesis

A

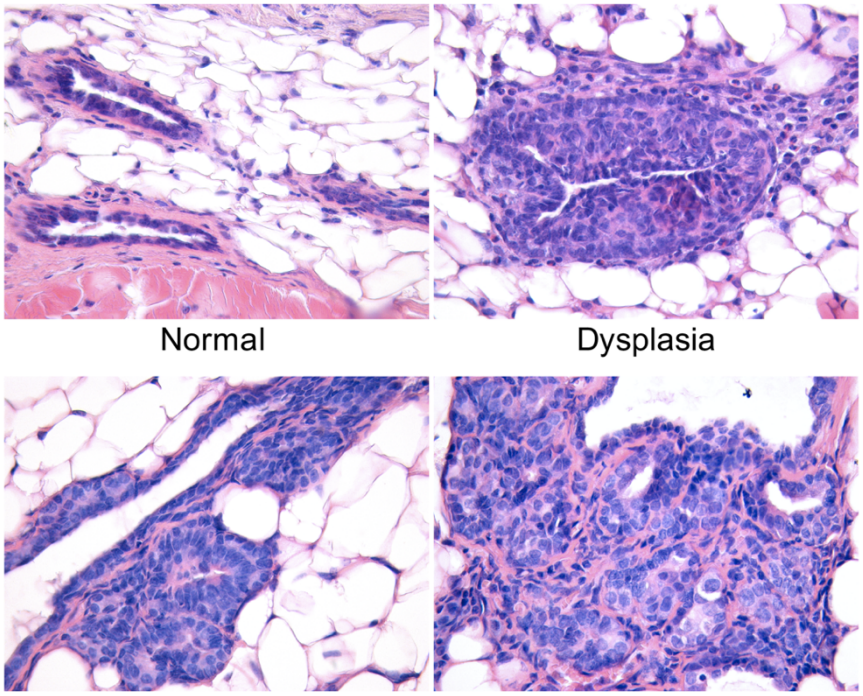

B

			Mammary glands											
ID	Sample	Mouse	Iperplasia (grado)	Iperplasia (estensione)	Infiltrato infiammatorio periduttale	Displasia (grado)	Displasia (estensione)	Carcinoma	Carcinoma (estensione)	Reazione stromale (grado)	Reazione stromale (estensione)	Flogosi del tessuto adiposo	score	Media score
AM 07	B/c + 6 w	11760	1	2	1	0	0	0	0	1	1	0	6	9
AM 09	B/c + 6 w	11762	2	2	2	2	2	0	0	1	1	0	12	
AM 11	B/c + 6 w	11764	2	2	2	1	1	0	0	1	2	0	11	
AM 15	B/c + 6 w	12197	2	2	1	2	1	0	0	1	1	0	10	
AM 16	B/c + 6 w	12198	1	2	1	1	1	0	0	1	2	0	9	
AM 17	B/c + 6 w	12199	1	3	2	1	2	0	0	1	2	0	12	
AN84	B/c + 6 w	14197	1	1	2	1	1	0	0	0	0	0	6	
AN85	B/c + 6 w	14200	2	2	2	1	2	0	0	2	1	0	12	
AN86	B/c + 6 w	14205	1	2	0	0	0	0	0	0	0	0	3	
AM 06	Neu T + 6 w	11759	2	2	1	3	2	2	1	0	0	0	13	13,44
AM 08	NeuT + 6 w	11761	2	2	2	3	2	1	1	1	1	3	18	
AM 10	NeuT + 6 w	11763	1	2	1	3	1	2	1	2	1	0	14	
AM 12	NeuT + 6 w	12159	2	2	2	1	1	0	0	1	2	0	11	
AM 13	NeuT + 6 w	12160	1	1	3	3	2	1	1	2	2	1	17	
AM 14	NeuT + 6 w	12161	2	2	1	2	2	0	0	1	2	0	12	
AN81	NeuT + 6 w	14198	2	2	2	3	2	0	0	2	2	0	15	
AN82	NeuT + 6 w	14202	2	2	1	3	2	1	2	2	1	0	16	
AN83	NeuT + 6 w	14204	1	1	1	1	1	0	0	0	0	0	5	

C

			Mammary glands											
ID	Sample	Mouse	Iperplasia (grado)	Iperplasia (estensione)	Infiltrato infiammatorio periduttale	Displasia (grado)	Displasia (estensione)	Carcinoma	Carcinoma (estensione)	Reazione stromale (grado)	Reazione stromale (estensione)	Flogosi del tessuto adiposo	score	Media score
AM30	B/c 12 w	11765	2	2	1	1	1	0	0	1	1	0	9	6,8
AM31	B/c 12 w	11770	2	2	1	1	1	0	0	1	1	0	9	
AM32	B/c 12 w	11752	1	1	1	0	0	0	0	0	0	0	3	
AO35	B/c 12 w	15652	1	2	1	0	0	0	0	2	2	0	8	
AO36	B/c 12 w	15653	1	2	1	0	0	0	0	1	2	0	7	
AO37	B/c 12 w	15654	2	2	1	0	0	0	0	2	2	0	9	
AO38	B/c 12 w	15657	1	1	1	0	0	0	0	1	1	0	5	
AM68	B/c 12 w		1	1	1	0	0	0	0	1	1	0	5	
AM69	B/c 12 w		1	1	1	0	0	0	0	1	1	1	6	
AM70	B/c 12 w		1	2	1	0	0	0	0	1	2	0	7	
AM27	NeuT + 12 w	11766	2	3	3	3	3	3	2	2	2	0	23	19,1
AM28	NeuT + 12 w	11769	2	3	1	3	3	3	1	2	2	1	21	
AM29	NeuT + 12 w	11771	2	3	1	3	3	1	2	2	2	0	19	
AO31	NeuT +12w	15655	2	3	1	3	2	2	2	1	2	0	18	
AO32	NeuT +12w	15656	2	3	1	3	2	2	2	2	2	0	19	
AO33	NeuT +12w	15658	2	3	1	3	3	3	2	2	2	0	21	
AO34	NeuT +12w	15659	2	2	2	3	2	0	0	2	2	0	15	
AM65	NeuT +12w		3	2	2	3	2	1	2	1	2	0	18	
AM66	NeuT +12w		3	2	2	3	2	1	1	1	1	1	17	
AM67	NeuT +12w		3	2	3	3	2	1	2	2	2	0	20	

Figure 11: (a) Representative H&E staining showed the stage of disease progression. **(b,c)**: Semi-quantitative disease score of 6 and 12 weeks mammary lesions evaluated on H&E-stained sections. The overall disease score was calculated as the sum of the individual variables scores.

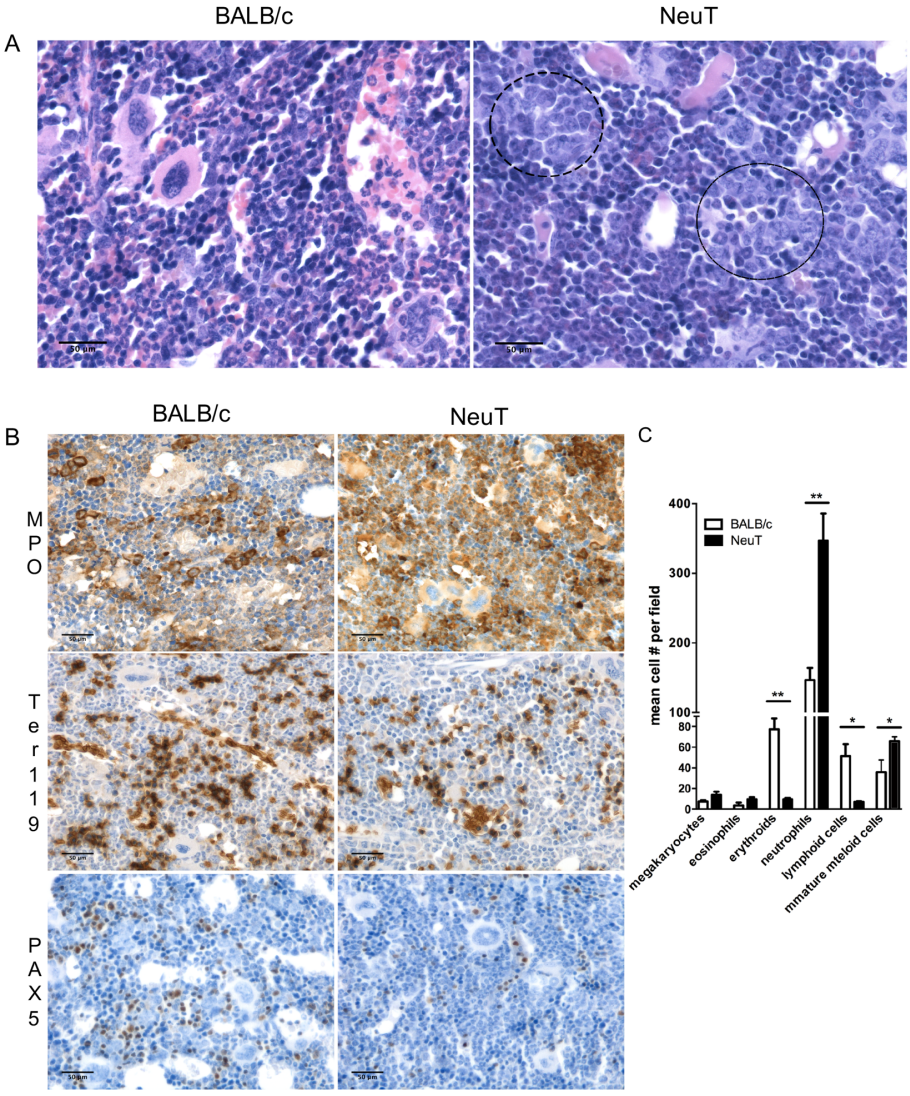

Figure 12: (a) A. Representative BM histology (H&E) of 24wks BALB/c and NeuT mice showing the increased density of immature myeloid granulocytic cell clusters and the contraction of erythroid and lymphoid elements in NeuT transgenic mice. Scale bars, 50 µm. A representative image is shown.
(b) Representative microphotographs of immunohistochemical stainings highlighting MPO+ myeloid elements, Ter119+ erythroid colonies and PAX5+ lymphoid B cells in 24wks BALB/c and NeuT BM sections. The immunostainings clearly indicate the expansion of myeloid elements and the concomitant contraction of the erythroid and B lymphoid populations. Scale bars, 50 µm. **(c)** Output of the quantitative analysis of BM hematopoietic composition based on cell counts performed on high-power microscopic fields (x400 magnifications) of H&E and immunostained sections.

5.6 Bone marrow hematopoietic adaptation is identified at pre-invasive and pre-malignant stages

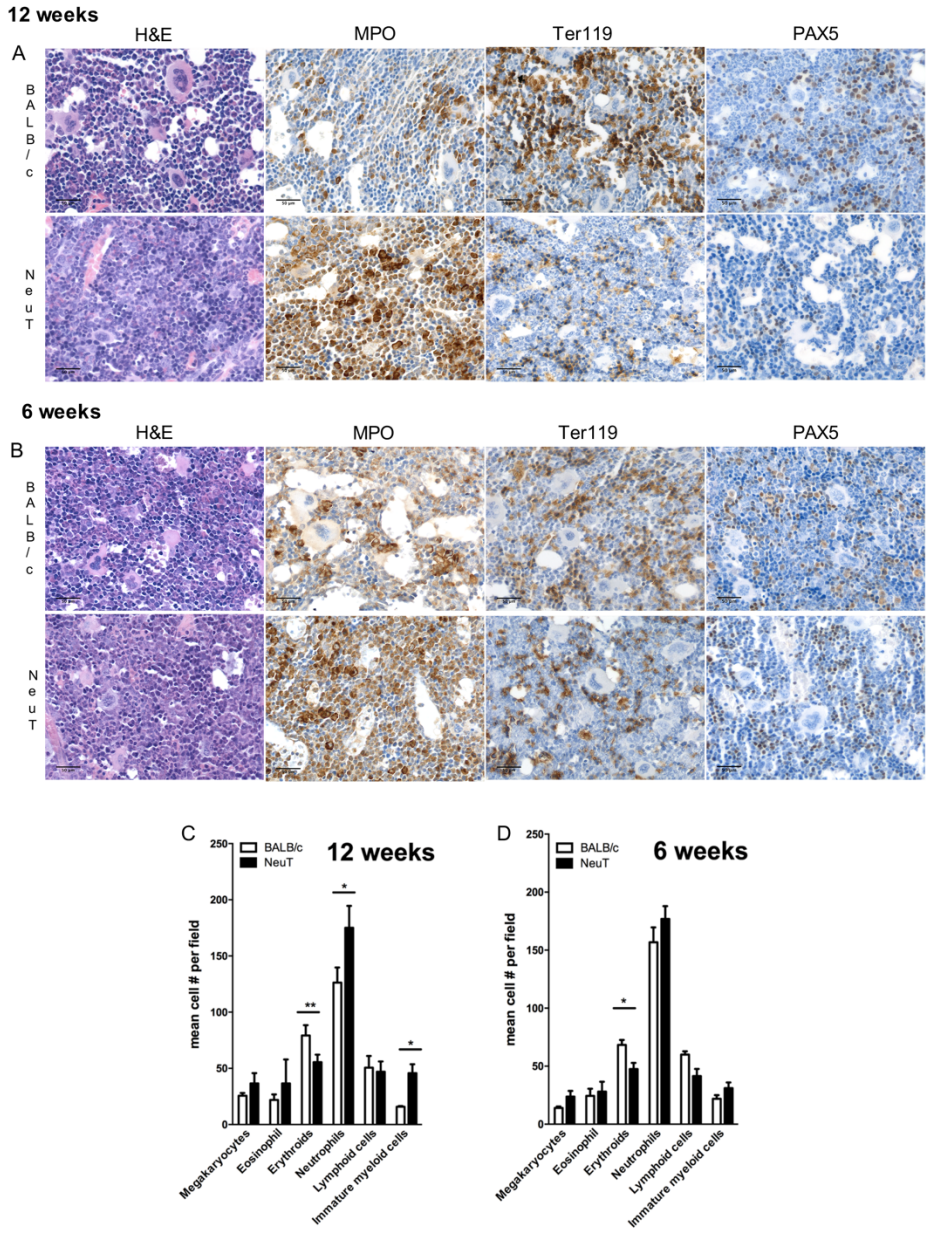

Figure 13: (a,b) Representative microphotographs of H&E histologies, MPO, Ter119 and PAX5 immunohistochemical stainings of 12wks **(a)** and 6wks **(b)** BALB/c and NeuT BM sections. The panel shows the relative increase of the density of MPO+ myeloid elements at the expenses of Ter119+ erythroid precursors and PAX5+ B lymphoid elements. Scale bars, 50 µm. **(c,d)** Output of the quantitative analysis of BM hematopoietic composition based on cell counts performed on high-power microscopic fields (x400 magnifications) of H&E and immunostained sections of 12 wks (**panel C**) and 6 wks (**panel D**) BALB/c and NeuT BM sections.

5.7 Bone marrow stromal architecture alterations at early stages of peripheral cancerogenesis

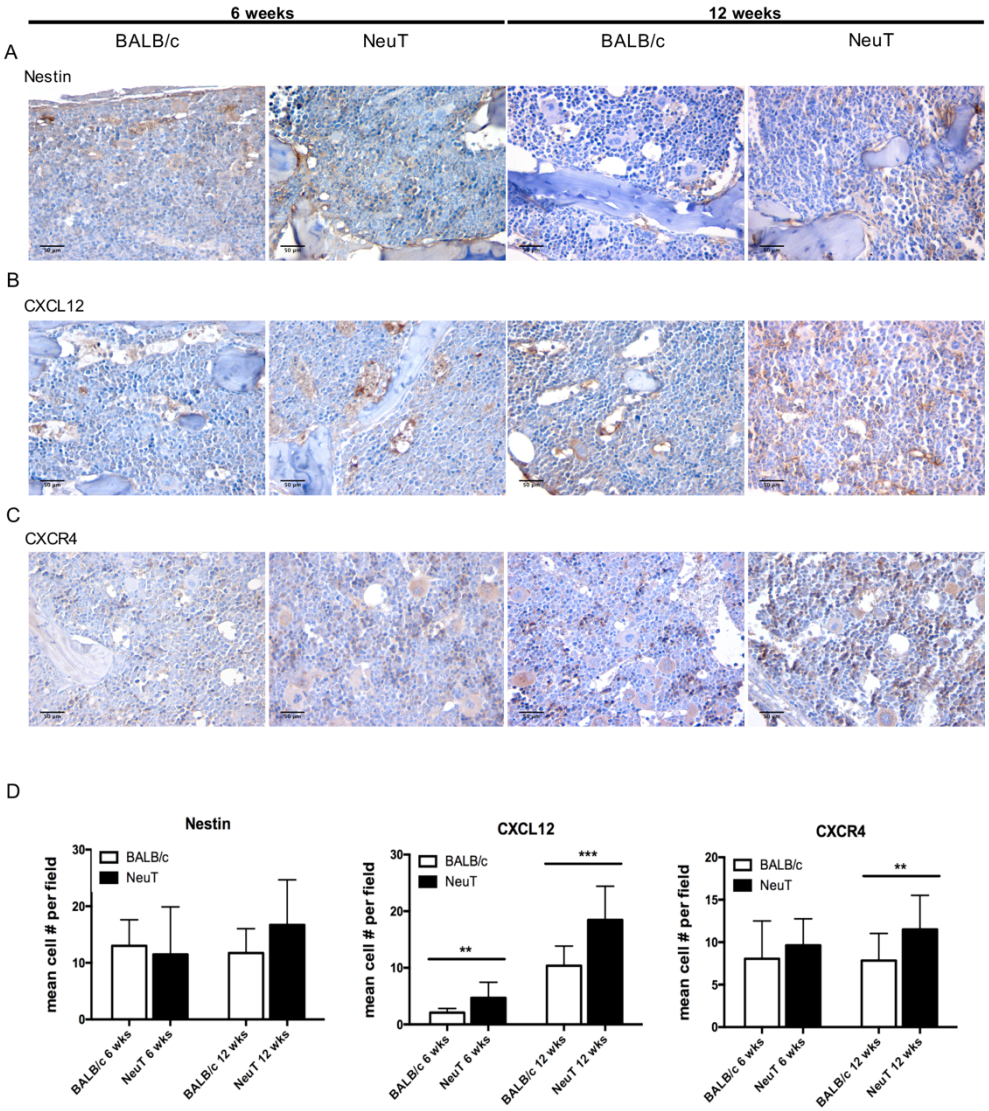

Figure 14: (a,b,c) Representative immunohistochemical stainings of Nestin+ mesenchymal stromal cells **(a)**, CXCL12 chemotactic stromal factor **(b)** and CXCR4 receptor **(c)** in BM sections of 6wks and 12wks BALB/c and NeuT mice showing the overall increase in the Nestin+ interstitial stromal meshwork in transgenic NeuT mice, the increase in CXCL12-expressing elements and the increase in CXCR4+ hematopoietic expression. Scale bars, 50 µm. **(d)** Quantitative immunolocalization analysis of Nestin, CXCL12 and CXCR4 on BM sections from 6w and 12w BALB/c and NeuT mice. The quantitative evaluation is expressed as the average percentage of marked areas calculated on software-segmented microphotographs from high-power microscopic fields (x400 magnifications)

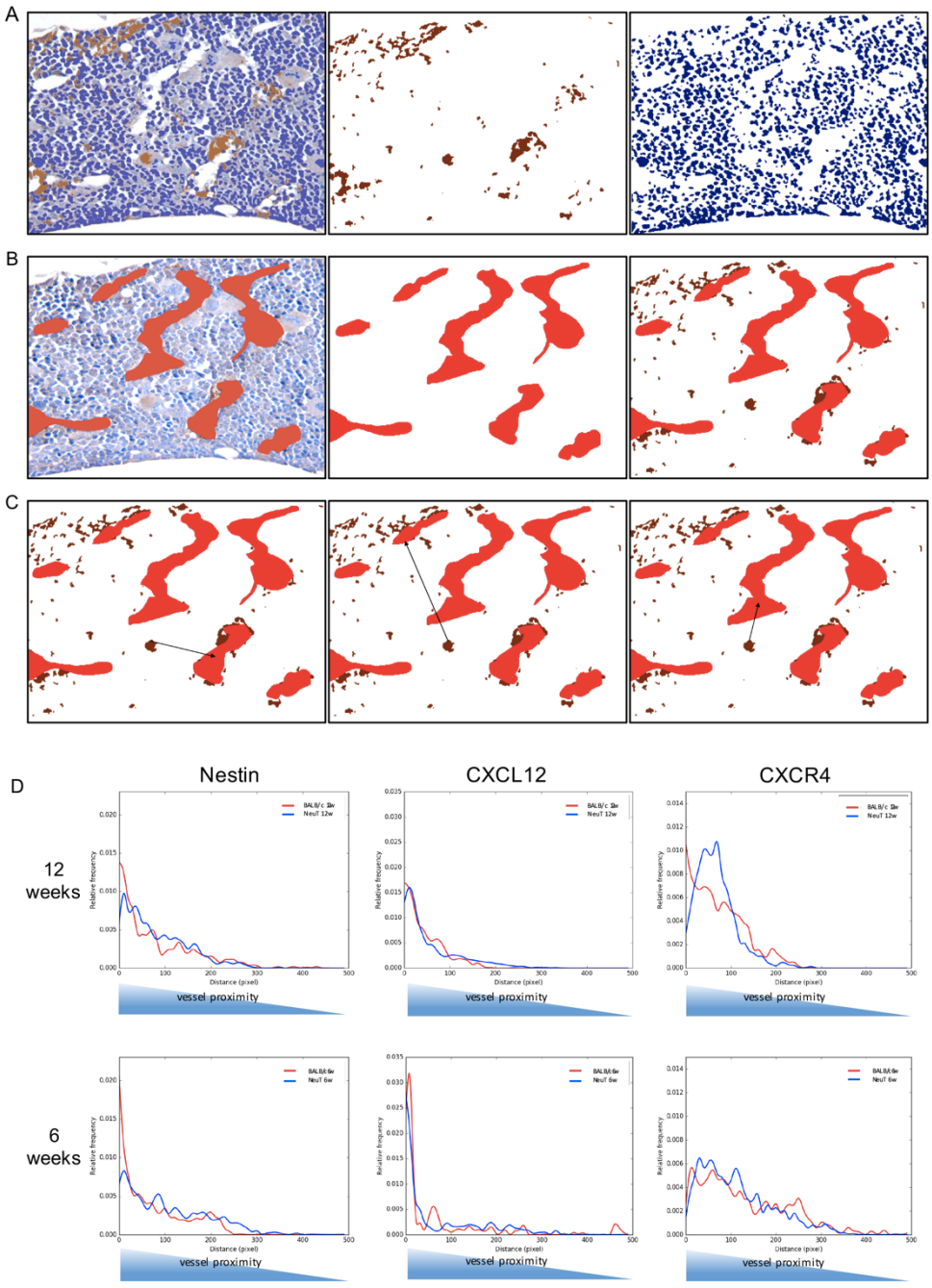

Figure 15: (a,b,c) Microphotographs segmentation evaluated the distances between IHC-labeled regions and selected regions of interest. The software calculated the number of pixels of the segmented IHC-labeled areas, and the minimum distance of each pixel from the selected regions of interest, creating a graph of distance distribution. Differences in the distance distribution of IHC markers from the selected regions of interest were calculated according to the Kolmogorov-Smirnov test.
(d) Vessel proximity distribution of Nestin, CXCL12 and CXCR4 in BM sections from 6 weeks and 12 weeks BALB/c and NeuT mice calculated on software-segmented microphotographs from high-power microscopic fields (x400 magnifications).

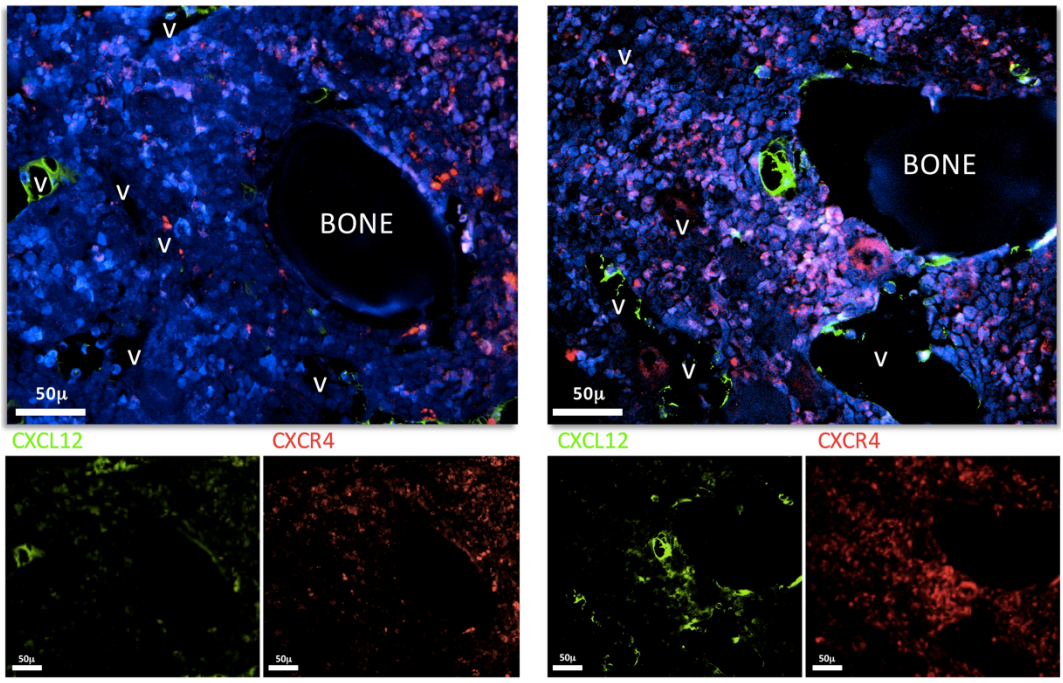

Figure 16: (a) Representative double-marker immunofluorescence showing CXCL12 (green signal) and CXCR4 (red signal) expression in the BM of 12w BALB/c and NeuT mice. The images highlight the overall induction and redistribution of CXCL12 and CXCR4 in the BM vascular area of transgenic mice.

Bibliography

(1): Wardle J, Robb K, Vernon S, Waller J. Screening for prevention and early diagnosis of cancer. Am Psychol. 2015 Feb-Mar;70(2):119-33. doi: 10.1037/a0037357. PubMed PMID: 25730719.

(2): Lorusso G, Rüegg C. The tumor microenvironment and its contribution to tumor evolution toward metastasis. Histochem Cell Biol. 2008 Dec;130(6):1091-103. doi: 10.1007/s00418-008-0530-8. Epub 2008 Nov 6. Review. PubMed PMID: 18987874.

(3): de Visser KE, Eichten A, Coussens LM. Paradoxical roles of the immune system during cancer development. Nat Rev Cancer. 2006 Jan;6(1):24-37. Review PubMed PMID: 16397525.

(4): Quail, D.F.; Joyce, J.A. Microenvironmental regulation of tumor progression and metastasis. *Nat. Med.* 2013, *19*, 1423–1437.

(5): Hanahan D, Coussens LM. Accessories to the crime: functions of cells recruited to the tumor microenvironment. Cancer Cell. 2012 Mar 20;21(3):309-22. doi:10.1016/j.ccr.2012.02.022. Review. PubMed PMID: 22439926.

(6): Albini A, Sporn MB. The tumour microenvironment as a target for chemoprevention. Nat Rev Cancer. 2007 Feb;7(2):139-47. Review. PubMed PMID:17218951.

(7): Medh RD, Thompson EB. Hormonal regulation of physiological cell turnover and apoptosis. Cell Tissue Res. 2000 Jul;301(1):101-24. Review. PubMed PMID:10928284; PubMed Central PMCID: PMC2763512.

(8): Kulkarni OP, Lichtnekert J, Anders HJ, Mulay SR. The Immune System in Tissue Environments Regaining Homeostasis after Injury: Is "Inflammation" Always Inflammation? Mediators Inflamm. 2016;2016:2856213. doi: 10.1155/2016/2856213. Epub 2016 Aug 11. Review. PubMed PMID: 27597803; PubMed Central PMCID:PMC4997018.

[9] Iwasaki A, Medzhitov R. Toll - like receptor control of the adaptive immune responses.Nat I mmunol. 2004;5(10):987 - 995.

(10): Sadik CD, Kim ND, Luster AD. Neutrophils cascading their way to inflammation. Trends Immunol. 2011;32(10):452 - 460.

(11): Shi C, Pamer EG. Monocyte recruitment during infection and inflammation. Nat Rev Immunol. 2011;11(11):762 - 774.

(12): Coussens LM, Werb Z. Inflammation and cancer. Nature. 2002 Dec 19-26;420(6917):860-7. Review. PubMed PMID: 12490959; PubMed Central PMCID:PMC2803035.

(13): Dibra D, Mishra L, Li S. Molecular mechanisms of oncogene-induced inflammation and inflammation-sustained oncogene activation in gastrointestinal tumors: an under-appreciated symbiotic relationship. Biochim Biophys Acta. 2014

Aug;1846(1):152-60. doi: 10.1016/j.bbcan.2014.05.001. Epub 2014 May 9. Review. PubMed PMID: 24821201; PubMed Central PMCID: PMC4140981
(14): Mantovani A, Allavena P, Sica A, Balkwill F. Cancer-related inflammation. Nature. 2008 Jul 24;454(7203):436-44. doi: 10.1038/nature07205. Review. PubMed PMID: 18650914.
(15): Giussani M, Merlino G, Cappelletti V, Tagliabue E, Daidone MG. Tumor-extracellular matrix interactions: Identification of tools associated with breast cancer progression. Semin Cancer Biol. 2015 Dec;35:3-10. doi:10.1016/j.semcancer.2015.09.012. Epub 2015 Sep 28. Review. PubMed PMID: 26416466.
(16): Tzanakakis G, Kavasi RM, Voudouri K, Berdiaki A, Spyridaki I, Tsatsakis A, Nikitovic D. Role of the extracellular matrix in cancer-associated epithelial to mesenchymal transition phenomenon. Dev Dyn. 2018 Mar;247(3):368-381. doi:10.1002/dvdy.24557. Epub 2017 Aug 30. Review. PubMed PMID: 28758355.
(17) Sangaletti S, Chiodoni C, Tripodo C, Colombo MP. Common extracellular matrix regulation of myeloid cell activity in the bone marrow and tumor microenvironments. Cancer Immunol Immunother. 2017 Aug;66(8):1059-1067. doi: 10.1007/s00262-017-2014-y. Epub 2017 May 13. Review. PubMed PMID: 28501940.
(18) Sangaletti S, Tripodo C, Santangelo A, Castioni N, Portararo P, Gulino A, Botti L, Parenza M, Cappetti B, Orlandi R, Tagliabue E, Chiodoni C, Colombo MP. Mesenchymal Transition of High-Grade Breast Carcinomas Depends on Extracellular Matrix Control of Myeloid Suppressor Cell Activity. Cell Rep. 2016 Sep 27;17(1):233-248. doi: 10.1016/j.celrep.2016.08.075. PubMed PMID: 27681434.
(19) Urb M, Sheppard DC. The role of mast cells in the defence against pathogens. PLoS Pathog. 2012;8(4):e1002619. doi: 10.1371/journal.ppat.1002619. Epub 2012 Apr 26. Review. PubMed PMID: 22577358; PubMed Central PMCID: PMC3343118.
(20) Amin K. The role of mast cells in allergic inflammation. Respir Med. 2012 Jan;106(1):9-14. doi: 10.1016/j.rmed.2011.09.007. Epub 2011 Nov 22. Review. PubMed PMID: 22112783.
(21) Frossi B, De Carli M, Pucillo C. The mast cell: an antenna of the microenvironment that directs the immune response. J Leukoc Biol. 2004 Apr;75(4):579-85. Epub 2004 Jan 14. Review. PubMed PMID: 14726495.
(22) Rao KN, Brown MA. Mast cells: multifaceted immune cells with diverse roles in health and disease. Ann N Y Acad Sci. 2008 Nov;1143:83-104. doi: 10.1196/annals.1443.023. Review. PubMed PMID: 19076346.
(23) Rigoni A, Colombo MP, Pucillo C. The Role of Mast Cells in Molding the Tumor Microenvironment. Cancer Microenviron. 2015 Dec;8(3):167-76. doi:10.1007/s12307-014-0152-8. Epub 2014 Sep 7. PubMed PMID: 25194694; PubMed Central PMCID: PMC4715001.
(24) Ribatti D, Crivellato E. Mast cells, angiogenesis, and tumour growth. Biochim Biophys Acta. 2012 Jan;1822(1):2-8. doi: 10.1016/j.bbadis.2010.11.010. Epub 2010 Dec 2. Review. PubMed PMID: 21130163.

(25) Huang B, Lei Z, Zhang GM, Li D, Song C, Li B, Liu Y, Yuan Y, Unkeless J, Xiong H, Feng ZH. SCF-mediated mast cell infiltration and activation exacerbate the inflammation and immunosuppression in tumor microenvironment. Blood. 2008 Aug 15;112(4):1269-79. doi: 10.1182/blood-2008-03-147033. Epub 2008 Jun 4. PubMed PMID: 18524989; PubMed Central PMCID: PMC2515142.
(26) Norrby K. Mast cells and angiogenesis. APMIS. 2002 May;110(5):355-71. Review. PubMed PMID: 12076253.
(27) Nielsen HJ, Hansen U, Christensen IJ, Reimert CM, Brünner N, Moesgaard F. Independent prognostic value of eosinophil and mast cell infiltration in colorectal cancer tissue. J Pathol. 1999 Dec;189(4):487-95. PubMed PMID:10629548.
(28) Kanbe N, Tanaka A, Kanbe M, Itakura A, Kurosawa M, Matsuda H. Human mast cells produce matrix metalloproteinase 9. Eur J Immunol. 1999 Aug;29(8):2645-9. PubMed PMID: 10458779.
(29) Almholt K, Johnsen M. Stromal cell involvement in cancer. Recent Results Cancer Res. 2003; 162:31-42. Review. PubMed PMID: 12790319.
(30) Lu LF, Lind EF, Gondek DC, Bennett KA, Gleeson MW, Pino-Lagos K, Scott ZA, Coyle AJ, Reed JL, Van Snick J, Strom TB, Zheng XX, Noelle RJ. Mast cells are essential intermediaries in regulatory T-cell tolerance. Nature. 2006 Aug 31;442(7106):997-1002. Epub 2006 Aug 20. PubMed PMID: 16921386.
(31) Danelli L, Frossi B, Gri G, Mion F, Guarnotta C, Bongiovanni L, Tripodo C, Mariuzzi L, Marzinotto S, Rigoni A, Blank U, Colombo MP, Pucillo CE. Mast cells boost myeloid-derived suppressor cell activity and contribute to the development of tumor-favoring microenvironment. Cancer Immunol Res. 2015 Jan;3(1):85-95. doi:10.1158/2326-6066.CIR-14-0102. Epub 2014 Oct 28. PubMed PMID: 25351848.
(32) Chow MT, Möller A, Smyth MJ. Inflammation and immune surveillance in cancer. Semin Cancer Biol. 2012 Feb;22(1):23-32. Doi 10.1016/j.semcancer.2011.12.004.Epub 2011 Dec 24. Review. PubMed PMID: 22210181
(33) Kumar S, Saini RV, Mahindroo N. Recent advances in cancer immunology and immunology-based anticancer therapies. Biomed Pharmacother. 2017 Dec;96:1491-1500. doi: 10.1016/j.biopha.2017.11.126. Epub 2017 Dec 2. Review. PubMed PMID: 29198747.
(34) Bauer CA, Kim EY, Marangoni F, Carrizosa E, Claudio NM, Mempel TR. Dynamic Treg interactions with intratumoral APCs promote local CTL dysfunction. J Clin Invest. 2014 Jun;124(6):2425-40. Doi10.1172/JCI66375. Epub 2014 May 8. PubMed PMID: 24812664; PubMed Central PMCID: PMC4089459.
(35) Pan PY, Ozao J, Zhou Z, Chen SH. Advancements in immune tolerance. Adv Drug Deliv Rev. 2008 Jan 14;60(2):91-105. Epub 2007 Oct 5. Review. PubMed PMID: 17976856; PubMed Central PMCID: PMC2228366.
(36) Nishikawa H, Sakaguchi S. Regulatory T cells in tumor immunity. Int J Cancer. 2010 Aug 15;127(4):759-67. doi: 10.1002/ijc.25429. Review. PubMed PMID: 20518016.

(37) Gabrilovich DI, Ostrand-Rosenberg S, Bronte V. Coordinated regulation of myeloid cells by tumours. Nat Rev Immunol. 2012 Mar 22;12(4):253-68. doi:10.1038/nri3175. Review. PubMed PMID: 22437938; PubMed Central PMCID: PMC3587148.
(38) Gabrilovich D. Mechanisms and functional significance of tumour-induced dendritic-cell defects. Nat Rev Immunol. 2004 Dec;4(12):941-52. Review. PubMed PMID: 15573129.
(39) Piccard H, Muschel RJ, Opdenakker G. On the dual roles and polarized phenotypes of neutrophils in tumor development and progression. Crit Rev Oncol Hematol. 2012 Jun;82(3):296-309. Doi 10.1016/j.critrevonc.2011.06.004. Epub 2011 Jul 27. Review. PubMed PMID: 21798756.
(40) Shizuru JA, Negrin RS, Weissman IL. Hematopoietic stem and progenitor cells: clinical and preclinical regeneration of the hematolymphoid system. Annu Rev Med.2005;56:509-38. Review. PubMed PMID: 15660525.Judith A. Shizuru 2005
(41) Akashi K, Traver D, Miyamoto T, Weissman IL. A clonogenic common myeloid progenitor that gives rise to all myeloid lineages. Nature. 2000 Mar 9;404(6774):193-7. PubMed PMID: 10724173.
(42) Orkin SH, Zon LI. Hematopoiesis: an evolving paradigm for stem cell biology.Cell. 2008 Feb 22;132(4):631-44. doi: 10.1016/j.cell.2008.01.025. PubMed PMID:18295580; PubMed Central PMCID: PMC2628169.
(43) Bianco P. Bone and the hematopoietic niche: a tale of two stem cells. Blood. 2011 May 19;117(20):5281-8. doi: 10.1182/blood-2011-01-315069. Epub 2011 Mar 15. Review. PubMed PMID: 21406722.
(44) Yin T, Li L. The stem cell niches in bone. J Clin Invest. 2006 May;116(5):1195-201. Review. PubMed PMID: 16670760; PubMed Central PMCID:PMC1451221.
(45) Sangaletti S, Tripodo C, Portararo P, Dugo M, Vitali C, Botti L, Guarnotta C, Cappetti B, Gulino A, Torselli I, Casalini P, Chiodoni C, Colombo MP. Stromal niche communalities underscore the contribution of the matricellular protein SPARC to B-cell development and lymphoid malignancies. Oncoimmunology. 2014 Jun 5;3:e28989. eCollection 2014. PubMed PMID: 25083326; PubMed Central PMCID: PMC4108469.
(46) Sahin AO, Buitenhuis M. Molecular mechanisms underlying adhesion and migration of hematopoietic stem cells. Cell Adh Migr. 2012 Jan-Feb;6(1):39-48. doi:10.4161/cam.18975. Review. PubMed PMID: 22647939; PubMed Central PMCID:PMC3364136.
(47) Wu WC, Sun HW, Chen HT, Liang J, Yu XJ, Wu C, Wang Z, Zheng L. Circulating hematopoietic stem and progenitor cells are myeloid-biased in cancer patients. Proc Natl Acad Sci U S A. 2014 Mar 18;111(11):4221-6. doi: 10.1073/pnas.1320753111. Epub 2014 Mar 3. PubMed PMID: 24591638; PubMed Central PMCID: PMC3964061.
(48) 1: Mitroulis I, Kalafati L, Hajishengallis G, Chavakis T. Myelopoiesis in the Context of Innate Immunity. J Innate Immun. 2018 Jun 6:1-8. doi: 10.1159/000489406. [Epub ahead of print] Review. PubMed PMID: 29874678.

(49) Sica A, Bronte V. Altered macrophage differentiation and immune dysfunction in tumor development. J Clin Invest. 2007 May;117(5):1155-66. Review. PubMed PMID: 17476345; PubMed Central PMCID: PMC1857267.
(50) Kumar V, Patel S, Tcyganov E, Gabrilovich DI. The Nature of Myeloid-Derived Suppressor Cells in the Tumor Microenvironment. Trends Immunol. 2016 Mar;37(3):208-220. doi: 10.1016/j.it.2016.01.004. Epub 2016 Feb 6. Review. PubMed PMID: 26858199; PubMed Central PMCID: PMC4775398.
(51) 1: Solito S, Bronte V, Mandruzzato S. Antigen specificity of immune suppression by myeloid-derived suppressor cells. J Leukoc Biol. 2011 Jul;90(1):31-6. doi: 10.1189/jlb.0111021. Epub 2011 Apr 12. Review. PubMed PMID: 21486906.
(52) Murdoch C, Muthana M, Coffelt SB, Lewis CE. The role of myeloid cells in the promotion of tumour angiogenesis. Nat Rev Cancer. 2008 Aug;8(8):618-31. doi: 10.1038/nrc2444. Epub 2008 Jul 17. Review. PubMed PMID: 18633355.
(53) Psaila B, Lyden D. The metastatic niche: adapting the foreign soil. Nat Rev Cancer. 2009 Apr;9(4):285-93. doi: 10.1038/nrc2621. Review. PubMed PMID:19308068; PubMed Central PMCID: PMC3682494.
(54) 1: Diaz-Montero CM, Salem ML, Nishimura MI, Garrett-Mayer E, Cole DJ, Montero AJ. Increased circulating myeloid-derived suppressor cells correlate with clinical cancer stage, metastatic tumor burden, and doxorubicin-cyclophosphamide chemotherapy. Cancer Immunol Immunother. 2009 Jan;58(1):49-59. doi: 10.1007/s00262-008-0523-4. Epub 2008 Apr 30. PubMed PMID: 18446337; PubMed Central PMCID: PMC3401888.
(55) Fleming V, Hu X, Weber R, Nagibin V, Groth C, Altevogt P, Utikal J, Umansky V. Targeting Myeloid-Derived Suppressor Cells to Bypass Tumor-Induced Immunosuppression. Front Immunol. 2018 Mar 2;9:398. doi:10.3389/fimmu.2018.00398. eCollection 2018. Review. PubMed PMID: 29552012; PubMed Central PMCID: PMC5840207.
(56) Greenberg NM, DeMayo F, Finegold MJ, Medina D, Tilley WD, Aspinall JO, Cunha GR, Donjacour AA, Matusik RJ, Rosen JM. Prostate cancer in a transgenic mouse. Proc Natl Acad Sci U S A. 1995 Apr 11;92(8):3439-43. PubMed PMID: 7724580; PubMed Central PMCID: PMC42182.
(57) Lucchini F, Sacco MG, Hu N, Villa A, Brown J, Cesano L, Mangiarini L, Rindi G, Kindl S, Sessa F, et al. Early and multifocal tumors in breast, salivary, harderian and epididymal tissues developed in MMTY-Neu transgenic mice. Cancer Lett. 1992 Jul 10;64(3):203-9. PubMed PMID: 1322235.
(58) Grimbaldeston MA, Chen CC, Piliponsky AM, Tsai M, Tam SY, Galli SJ. Mast cell-deficient W-sash c-kit mutant Kit W-sh/W-sh mice as a model for investigating mast cell biology in vivo. Am J Pathol. 2005 Sep;167(3):835-48. PubMed PMID: 16127161; PubMed Central PMCID: PMC1698741.
(59) Boggio K, Nicoletti G, Di Carlo E, Cavallo F, Landuzzi L, Melani C, Giovarelli M, Rossi I, Nanni P, De Giovanni C, Bouchard P, Wolf S, Modesti A, Musiani P, Lollini PL, Colombo MP, Forni G. Interleukin 12-mediated prevention of spontaneous

mammary adenocarcinomas in two lines of Her-2/neu transgenic mice. J Exp Med. 1998 Aug 3;188(3):589-96. PubMed PMID: 9687535; PubMed Central PMCID:PMC2212479.
(60) Pittoni P, Tripodo C, Piconese S, Mauri G, Parenza M, Rigoni A, Sangaletti S, Colombo MP. Mast cell targeting hampers prostate adenocarcinoma development but promotes the occurrence of highly malignant neuroendocrine cancers. Cancer Res. 2011 Sep 15;71(18):5987-97. doi: 10.1158/0008-5472.CAN-11-1637. Epub 2011 Sep 6. PubMed PMID: 21896641.
(61) 1: Shappell SB, Thomas GV, Roberts RL, Herbert R, Ittmann MM, Rubin MA, Humphrey PA, Sundberg JP, Rozengurt N, Barrios R, Ward JM, Cardiff RD. Prostate pathology of genetically engineered mice: definitions and classification. The consensus report from the Bar Harbor meeting of the Mouse Models of Human Cancer Consortium Prostate Patholog Committee. Cancer Res. 2004 Mar 15;64(6):2270-305. Review. PubMed PMID: 15026373.
(62) Chiaverotti T, Couto SS, Donjacour A, Mao JH, Nagase H, Cardiff RD, Cunha GR, Balmain A. Dissociation of epithelial and neuroendocrin carcinoma lineages in the transgenic adenocarcinoma of mouse prostate model of prostate cancer. Am J Pathol. 2008 Jan;172(1):236-46. Epub 2007 Dec 21. PubMed PMID: 18156212; PubMed Central PMCID: PMC2189611.
(63) Leong KG, Wang BE, Johnson L, Gao WQ. Generation of a prostate from a single adult stem cell. Nature. 2008 Dec 11;456(7223):804-8. doi: 10.1038/nature07427. Epub 2008 Oct 22. PubMed PMID: 18946470.
(64) Quintás-Cardama A, Kantarjian H, Cortes J. Imatinib and beyond--exploring the full potential of targeted therapy for CML. Nat Rev Clin Oncol. 2009 Sep;6(9):535-43. doi: 10.1038/nrclinonc.2009.112. Epub 2009 Aug 4. Review. PubMed PMID: 19652654.
(65) 1: Joensuu H, DeMatteo RP. The management of gastrointestinal stromal tumors: a model for targeted and multidisciplinary therapy of malignancy. Annu Rev Med. 2012;63:247-58. doi: 10.1146/annurev-med-043010-091813. Epub 2011 Oct 13. Review. PubMed PMID: 22017446; PubMed Central PMCID: PMC3381421.
(66) Druker BJ, Tamura S, Buchdunger E, Ohno S, Segal GM, Fanning S, Zimmermann J, Lydon NB. Effects of a selective inhibitor of the Abl tyrosine kinase on the growth of Bcr-Abl positive cells. Nat Med. 1996 May;2(5):561-6. PubMed PMID: 8616716.
(67) Buchdunger E, Cioffi CL, Law N, Stover D, Ohno-Jones S, Druker BJ, Lydon NB. Abl protein-tyrosine kinase inhibitor STI571 inhibits in vitro signal transduction mediated by c-kit and platelet-derived growth factor receptors. JPharmacol Exp Ther. 2000 Oct;295(1):139-45. PubMed PMID: 10991971.
(68) 1: Bronte V, Brandau S, Chen SH, Colombo MP, Frey AB, Greten TF, Mandruzzato S, Murray PJ, Ochoa A, Ostrand-Rosenberg S, Rodriguez PC, Sica A, Umansky V, Vonderheide RH, Gabrilovich DI. Recommendations for myeloid-derived suppressor cell nomenclature and characterization standards. Nat Commun. 2016 Jul

6;7:12150. doi: 10.1038/ncomms12150. Review. PubMed PMID: 27381735; PubMed Central PMCID: PMC4935811.
(69) Saleem SJ, Martin RK, Morales JK, Sturgill JL, Gibb DR, Graham L, Bear HD, Manjili MH, Ryan JJ, Conrad DH. Cutting edge: mast cells critically augment myeloid-derived suppressor cell activity. J Immunol. 2012 Jul 15;189(2):511-5. doi: 10.4049/jimmunol.1200647. Epub 2012 Jun 15. PubMed PMID: 22706087; PubMed Central PMCID: PMC3392490.
(70) Pan PY, Ma G, Weber KJ, Ozao-Choy J, Wang G, Yin B, Divino CM, Chen SH. Immune stimulatory receptor CD40 is required for T-cell suppression and T regulatory cell activation mediated by myeloid-derived suppressor cells in cancer. Cancer Res. 2010 Jan 1;70(1):99-108. doi: 10.1158/0008-5472.CAN-09-1882. Epub 2009 Dec 8. PubMed PMID: 19996287; PubMed Central PMCID: PMC2805053.

Scientific Products:

Discussed in this thesis:

- Myeloid Derived Suppressor Cells-Mast Cells Cross-Talk Via CD40- CD40L Mediates Tumor Specific Immunosuppression in Prostate Cancer. Jachetti E, **Cancila V**, Rigoni A, Bongiovanni L, Cappetti B, Belmonte B, Enriquez C, Casalini P, Ostano P, Frossi B, Sangaletti S, Chiodoni C, Chiorino G, Pucillo CE, Tripodo C, Colombo MP. Cancer Immunol Res

- Imatinib spares cKit-expressing prostate neuroendocrine tumors, whereas kills seminal vescicle epithelial-stromal tumors by targeting PDGFR-beta. Jachetti E, Rigoni A, Bongiovanni L, Arioli I, Botti L, Parenza M, **Cancila V**, Chiodoni C, Festinese F, Bellone M, Tardanico R, Tripodo C, Colombo MP. Mol Cancer Ther. 2017 Feb; 16(2):365-375. doi: 10.1158/1535-7163.MCT-16-0466. Epub 2016 Dec 15. PubMed PMID: 28600479

- Bone marrow hematopoietic adaptation to distant incipient cancer implies an inflammatory transcriptional switch and stromal rearrangement *Paper in submission*

Not included in this thesis:

- Fortunato O, Borzi C, Milione M, Centonze G, Conte D, Boeri M, Verri C, Moro M, Facchinetti F, Andriani F, Roz L, Caleca L, Huber V, Cova A, Camisaschi C, Castelli C, **Cancila V**, Tripodo C, Pastorino U, Sozzi G. Circulating mir-320° promotes immunosuppressive macrophages M2 phenotype associated with lung cancer risk. Int J Cancer. 2018 Nov 13. doi: 10.1002/ijc.31988. [Epub ahead of print] PubMed PMID: 30426475.

- Di Napoli A, De Cecco L, Piccaluga PP, Navari M, **Cancila V**, Cippitelli C, Pepe G, Lopez G, Monardo F, Bianchi A, D'Amore ESG, Gianelli U, Facchetti F, Berti E, Bhagat G. Transcriptional analysis distinguishes breast implant-associated anaplastic large cell lymphoma from other peripheral T-cell lymphomas. Mod Pathol. 2018 Sep 11. doi: 10.1038/s41379-018-0130-7. [Epub ahead of print] PubMed PMID: 30206415.

- Lo Russo G, Moro M, Sommariva M, **Cancila V**, Boeri M, Centonze G, Ferro S, Ganzinelli M, Gasparini P, Huber V, Milione M, Porcu L, Proto C, Pruneri G, Signorelli D, Sangaletti S, Sfondrini L, Storti C, Tassi E, Bardelli A, MarsoniS, Torri V, Tripodo C, Colombo MP, Anichini A, Rivoltini L, Balsari A, Sozzi G, Garassino

M. Antibody-Fc/FcR Interaction on Macrophages as a Mechanism for Hyperprogressive Disease in Non-Small Cell Lung Cancer Subsequent to PD-1/PD-L1 Blockade. Clin Cancer Res. 2018 Sep 11. pii: clincanres.1390.2018. doi: 10.1158/1078-0432.CCR-18-1390. [Epub ahead of print] PubMed PMID: 30206165.

- Vacca D, **Cancila V**, Gulino A, Lo Bosco G, Belmonte B, Di Napoli A, Florena AM, Tripodo C, Arancio W. Real-time detection of BRAF V600E mutation from archival hairy cell leukemia FFPE tissue by nanopore sequencing. Mol Biol Rep. 2018 Feb;45(1):1-7. doi: 10.1007/s11033-017-4133-0. Epub 2017 Dec 13. PubMed PMID:29238890.

- Ratti C, Botti L, **Cancila V**, Galvan S, Torselli I, Garofalo C, Manara MC, Bongiovanni L, Valenti CF, Burocchi A, Parenza M, Cappetti B, Sangaletti S, Tripodo C, Scotlandi K, Colombo MP, Chiodoni C. Trabectedin Overrides Osteosarcoma Differentiative Block and Reprograms the Tumor Immune Environment Enabling Effective Combination with Immune Checkpoint Inhibitors. Clin Cancer Res. 2017 Sep 1;23(17):5149-5161. doi: 10.1158/1078-0432.CCR-16-3186. Epub 2017 Jun 9. PubMed PMID: 28600479.

- Emma MR, Iovanna JL, Bachvarov D, Puleio R, Loria GR, Augello G, Candido S, Libra M, Gulino A, **Cancila V**, McCubrey JA, Montalto G, Cervello M. NUPR1, a new target in liver cancer: implication in controlling cell growth, migration, invasion and sorafenib resistance. Cell Death Dis. 2016 Jun 23;7(6):e2269. doi: 10.1038/cddis.2016.175. PubMed PMID: 27336713; PubMed Central PMCID: PMC5143401.